

Neutrino emission from temporarily-absorbed gamma-ray blazars

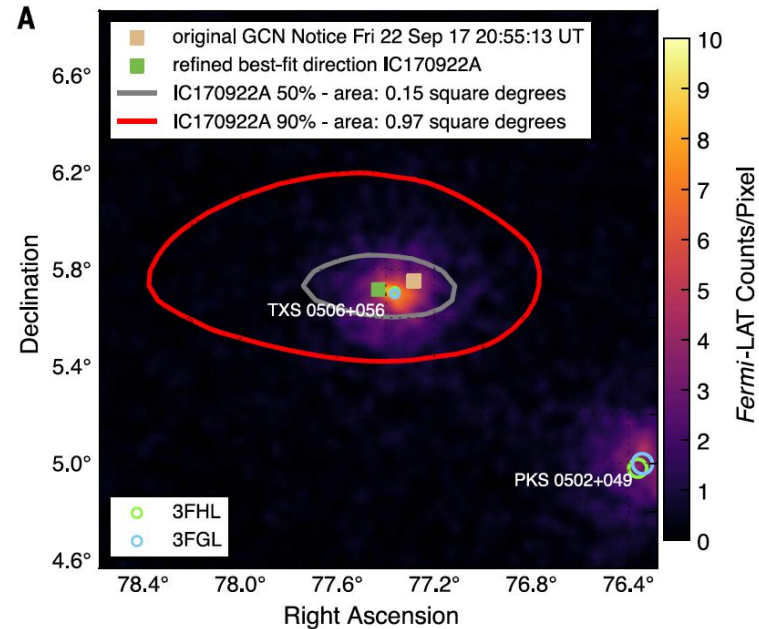
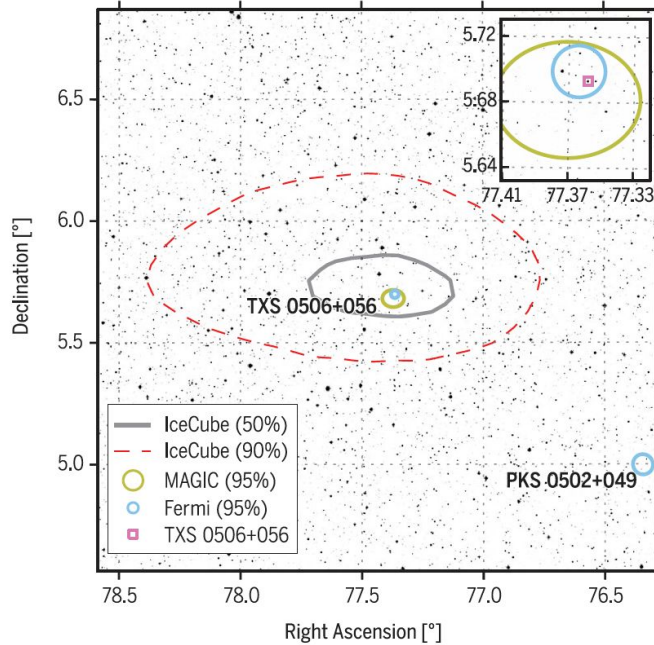
Presenter: Emma Kun (Konkoly Observatory, Budapest, Hungary)

EPS-HEP, 2021.07.09

Collaborators (alphabetical order)

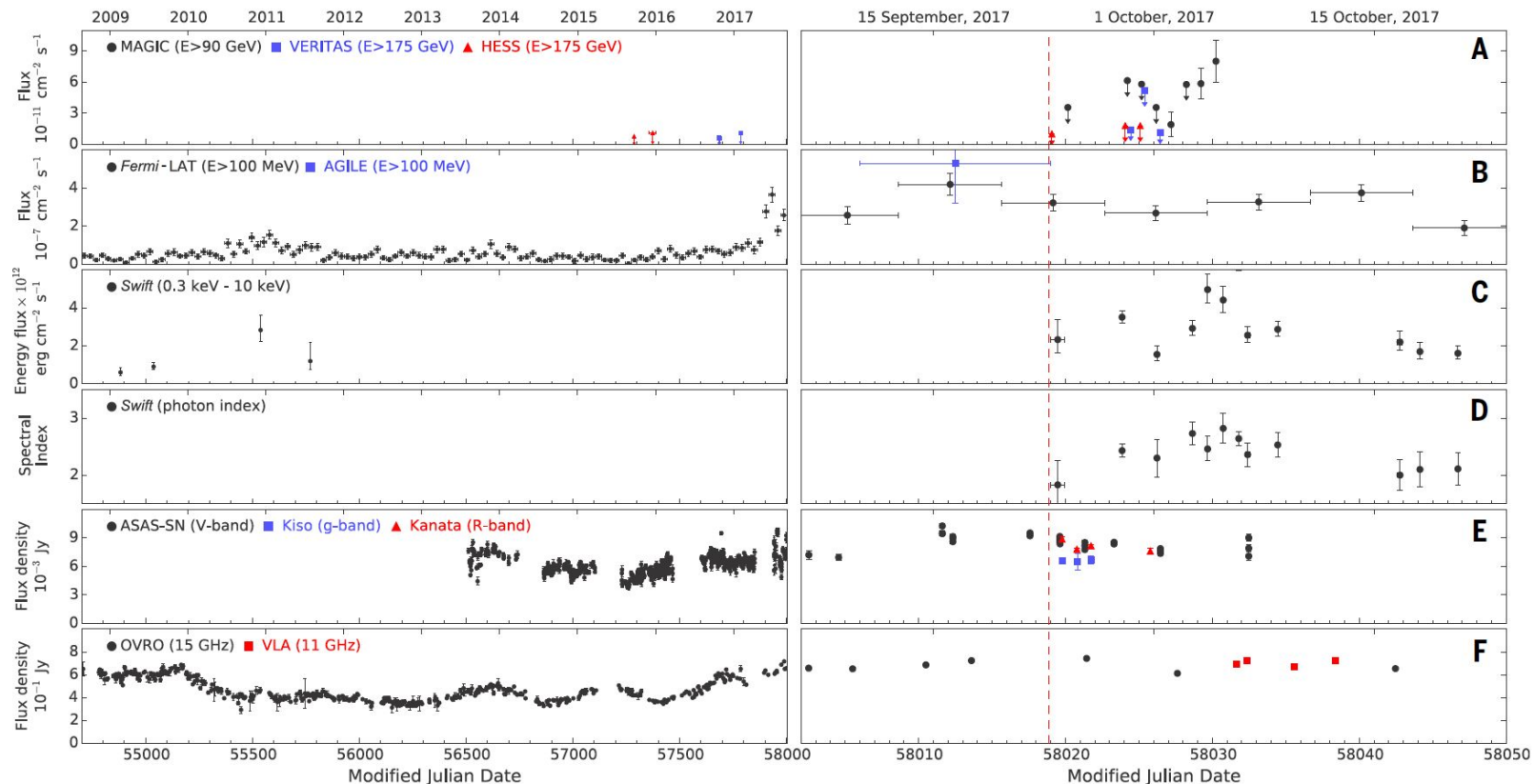
Imre Bartos, Julia Becker-Tjus, Peter L. Biermann, Francis Halzen, Emma Kun, Patrick Reichherzer, Marcel Schroller

TXS 0506+056 — identified high-energy neutrino source IceCube-170922A



Multimessenger observations

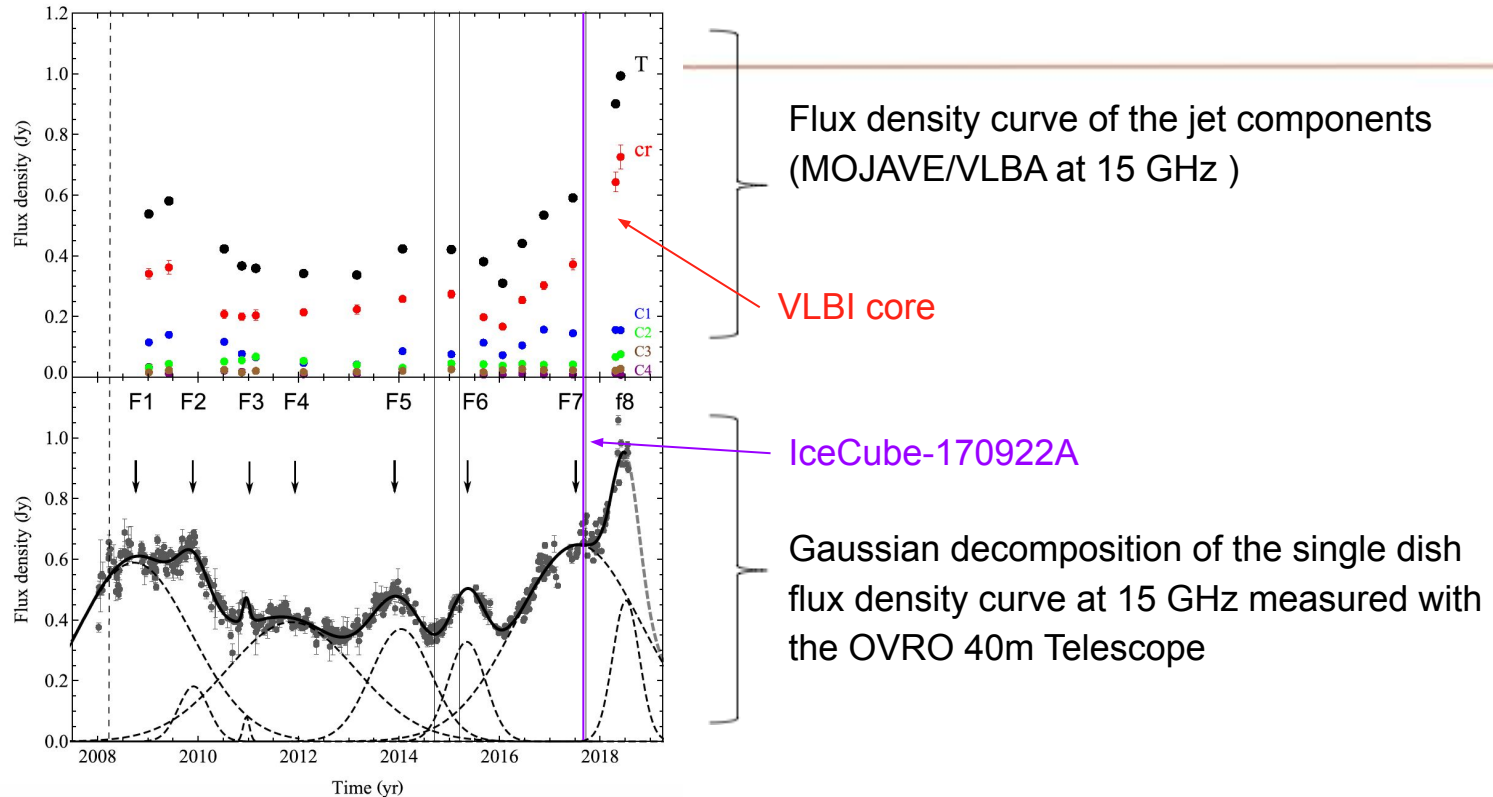
The IceCube Collaboration, Fermi-LAT, MAGIC, AGILE, ASAS-SN, HAWC, H.E.S.S., INTEGRAL, Kanata, Kiso, Kapteyn, Liverpool Telescope, Subaru, Swift/NuSTAR, VERITAS, and VLA/17B-403 teams, 2018, Science, 361, 6398



The IceCube Collaboration, Fermi-LAT, MAGIC, AGILE, ASAS-SN, HAWC, H.E.S.S, INTEGRAL, Kanata, Kiso, Kapteyn, Liverpool Telescope, Subaru, Swift/NuSTAR, VERITAS, and VLA/17B-403 teams, 2018, Science, 361, 6398

Radio brightening of TXS 0506+056

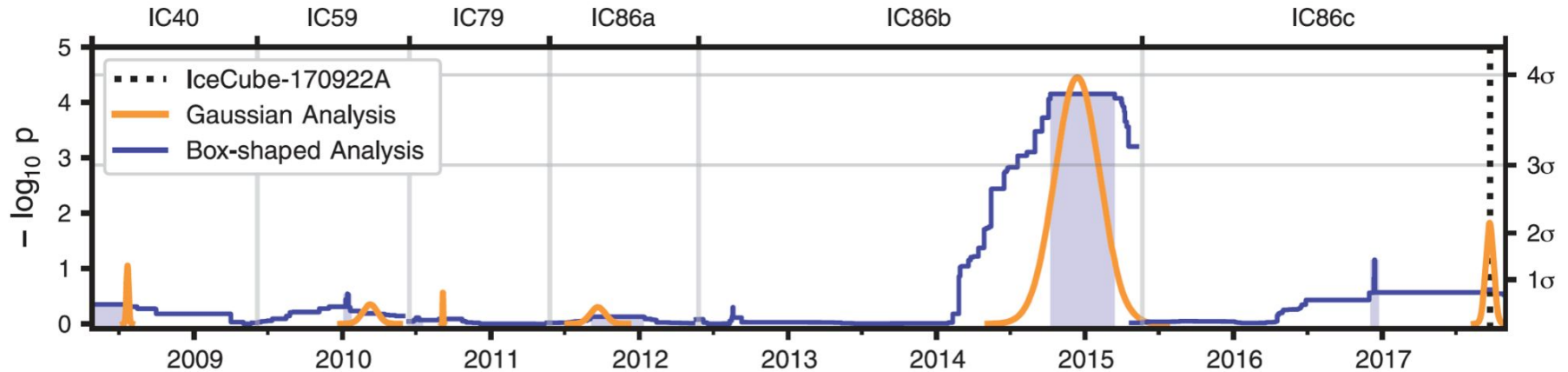
Kun, Biermann, Gergely 2019, MNRAS Letters, 483, 42



The VLBI core is responsible for the abrupt radio brightening of the source at 15 GHz

Same results at 43 GHz (Ros, Kadler, Perucho, et al. 2020, A&A, 633, L1)

Neutrino emission from the direction of the blazar TXS 0506+056 prior to the IceCube-170922A alert



The IceCube Collaboration found an excess of high-energy neutrino events between September 2014 and March 2015. Allowing for time-variable flux, this constitutes 3.5σ evidence for neutrino emission from the direction of TXS 0506+056, independent of and prior to the 2017 flaring episode.

IceCube Collaboration 2018, Science 361, 147-151

TXS 0506+056

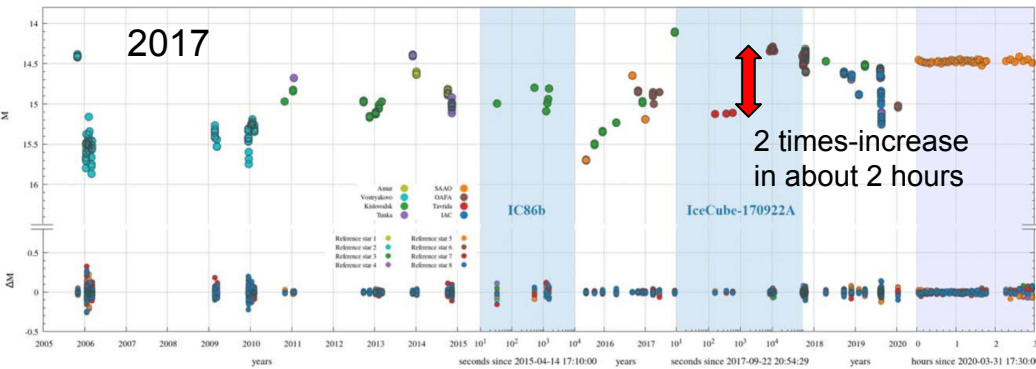
2014-15: no gamma-ray flare.

The long-term radio flare starts after that burst.

2017: the blazar was off at the time of the neutrino and then turned on as seen in the optical (MASTER), TeV gamma (MAGIC) and Fermi data.

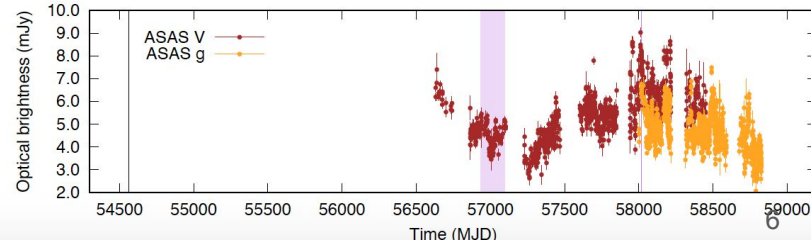
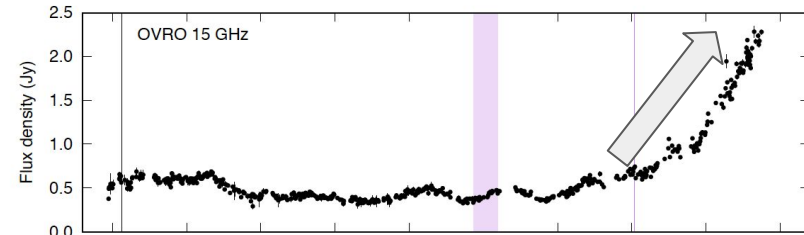
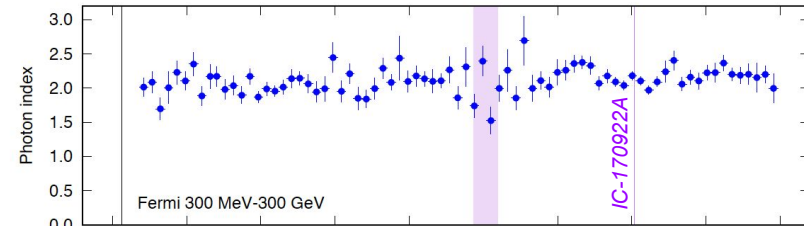
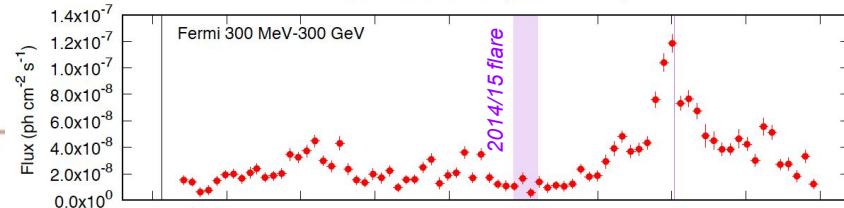
MASTER observations of TXS 0506+05

MASTER observations of TXS 0506+05



Lipunov et al. 2020, ApJ, 896, 19L

4FGL J0509.4+0542 (TXS 0506+056)

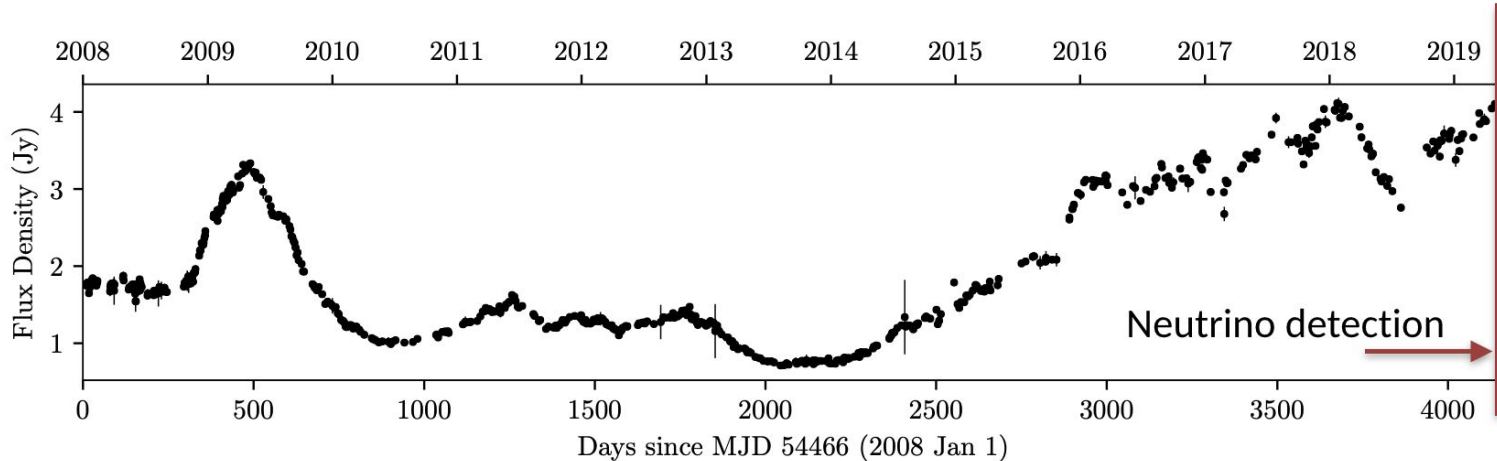


The plot is made to internal use

Neutrino candidate source FSRQ PKS 1502+106 at highest flux density at 15 GHz

IceCube detected a high-energy neutrino on 2019/07/30.86853

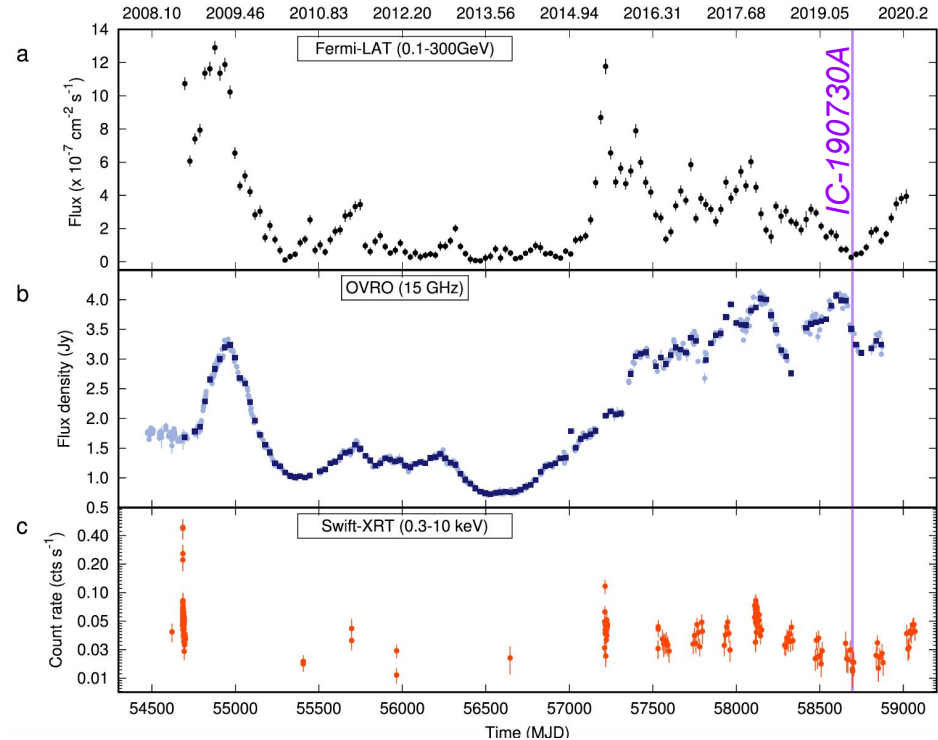
FSRQ PKS 1502+106 is located within the 50% uncertainty region of the event



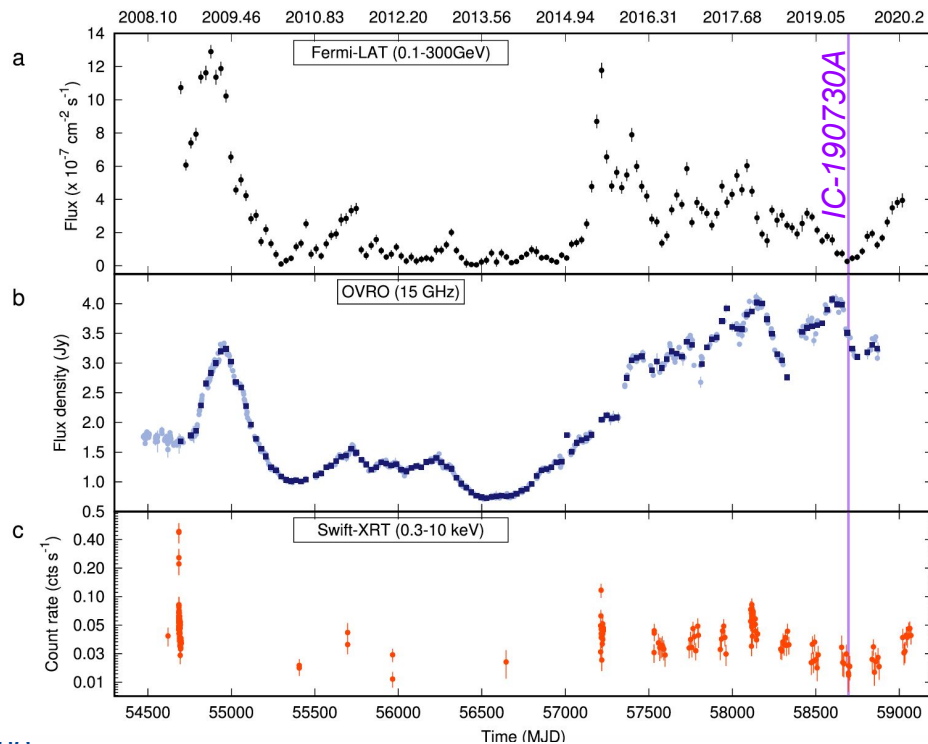
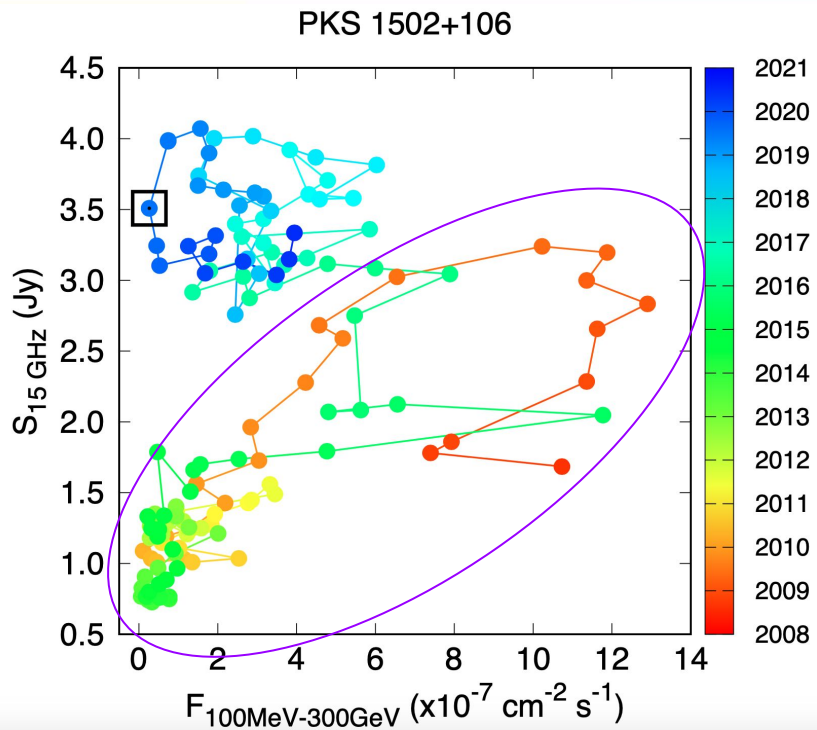
The flux density of FSRQ PKS 1502+106 at 15 GHz measured with the OVRO 40m Telescope show a long-term outburst, that reached its all-time maximum at about the neutrino was detected

Background

- What can gamma and radio data teach us about blazars and neutrinos?
- Catalogue searches and comparisons of OVRO radio flux densities and Fermi light curves
- PKS 1502+106: neutrino arrived in a deep gamma-minimum
- Likelihood analysis of Fermi data
- Dedicated project on a cluster of 16x2.2 GHz Intel Skylake vCPUs (PI: EK; Parent cluster: ELKH Cloud, Wigner Data Center, Hungary)



PKS 1502+106: gamma-ray flux vs radio flux density



Mode1: gamma correlates with radio, the radio lagging behind the gamma flux ($R=0.85$, $\tau_c=59+32$ days)

Mode2: more complex connection

What caused this switch?

Three famous cases, when a neutrino arrived in at least a local, for PKS in a global gamma-minimum

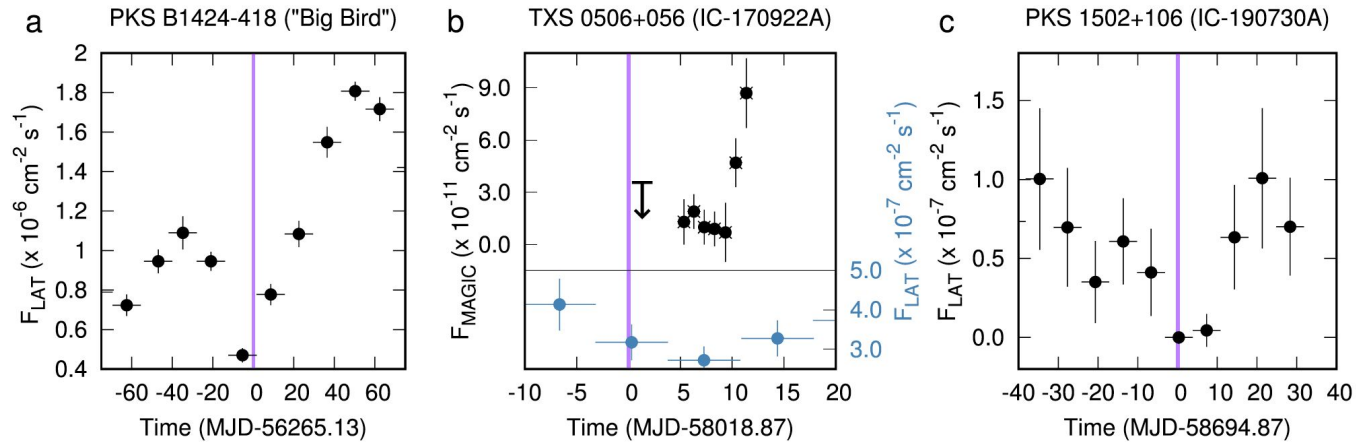
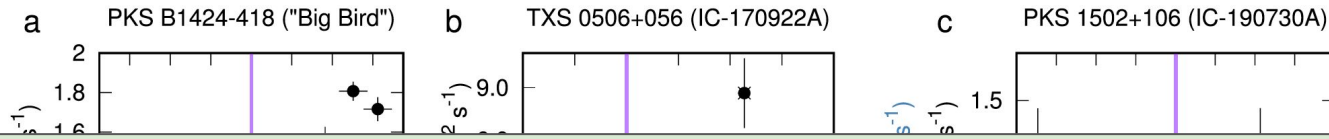


Figure 3. γ -ray light curves for three blazars with coincident high-energy neutrinos. (a) PKS B1424-418 as measured by Fermi-LAT (100 MeV–300 GeV, 14 day binning), plotted by black dots with error bars (Kadler et al. 2016). The vertical purple line marks the detection time of the neutrino event HESE 35. (b) The very-high-energy γ -ray light curve of TXS 0506+056 as measured by MAGIC ($E > 90$ GeV), plotted by black dots with error bars, and the high-energy γ -ray light curve of TXS 0506+056 as measured by Fermi ($E > 100$ MeV, 7 days binning), plotted by blue dots with error bars (IceCube Collaboration et al. 2018). The vertical purple line marks the detection time of the neutrino event IC-170922A. (c) Fermi-LAT γ -ray light curve of PKS 1502+106 (100 MeV–300 GeV, 7 days binning), plotted by black dots with error bars. The vertical purple line marks the detection time of the neutrino event IC-190730A. The arrival time of the neutrinos sets the zero value on the time axis of the plots.

Kun, Bartos, Becker-Tjus, Biermann, Halzen, Mező, 2021, ApJL, 911, L18

Three famous cases, when a neutrino arrived in at least a local, for PKS in a global gamma-minimum



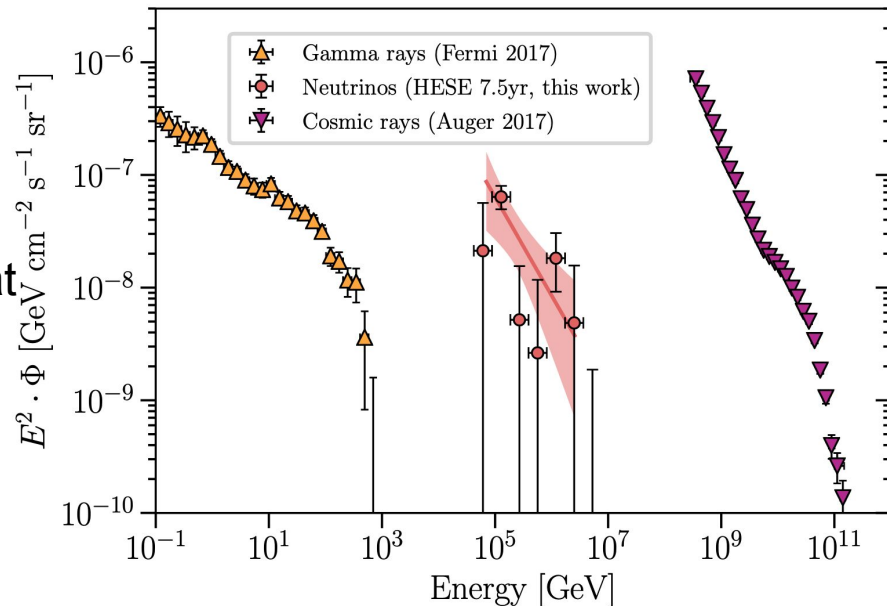
Temporal γ -suppression potentially resolves the apparent contradiction of the blazar models simultaneously producing a detectable neutrino flux and a gamma flare, since at the time of efficient neutrino production the observed gamma-flux drops.

Figure 3. γ -ray light curves for three blazars with coincident high-energy neutrinos. (a) PKS B1424-418 as measured by Fermi-LAT (100 MeV–300 GeV, 14 day binning), plotted by black dots with error bars (Kadler et al. 2016). The vertical purple line marks the detection time of the neutrino event HESE 35. (b) The very-high-energy γ -ray light curve of TXS 0506+056 as measured by MAGIC ($E > 90$ GeV), plotted by black dots with error bars, and the high-energy γ -ray light curve of TXS 0506+056 as measured by Fermi ($E > 100$ MeV, 7 days binning), plotted by blue dots with error bars (IceCube Collaboration et al. 2018). The vertical purple line marks the detection time of the neutrino event IC-170922A. (c) Fermi-LAT γ -ray light curve of PKS 1502+106 (100 MeV–300 GeV, 7 days binning), plotted by black dots with error bars. The vertical purple line marks the detection time of the neutrino event IC-190730A. The arrival time of the neutrinos sets the zero value on the time axis of the plots.

Kun, Bartos, Becker-Tjus, Biermann, Halzen, Mező, 2021, ApJL, 911, L18

High-energy fluxes of gamma rays, neutrinos, and cosmic rays

- Similar power-law energetics, Γ_v : 2.3-2.9
- Contribution to the specific messenger:
 - Gamma-rays: blazars~80%
 - Neutrinos: blazars<30%
- More flux in neutrinos at lower energies than could be expected from gamma-rays, *if* they have the same sources.
- There could be a population of neutrino sources, that are obscured in gamma-rays

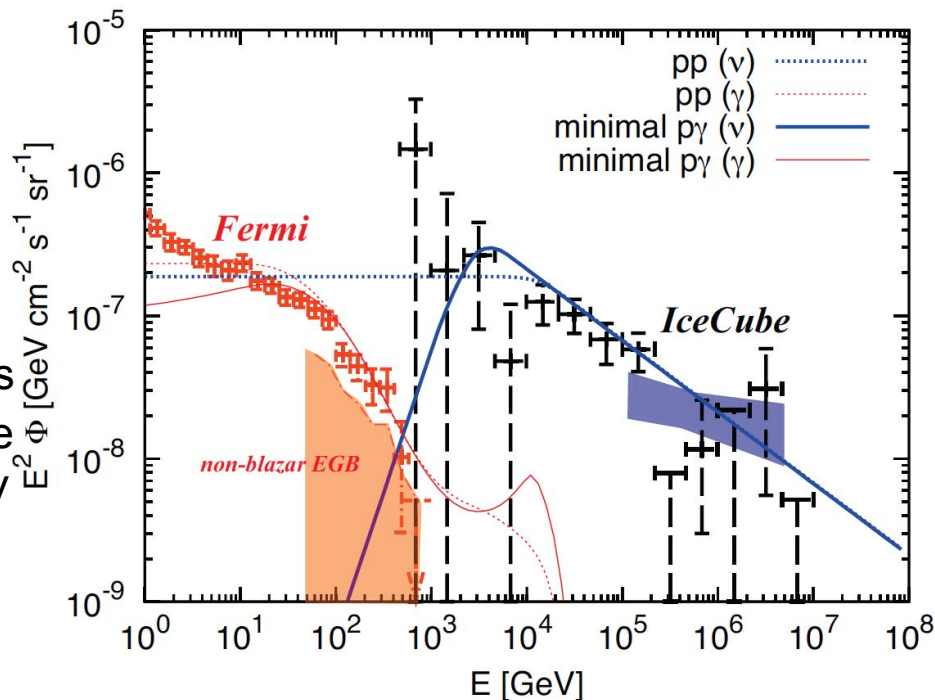


The IceCube high-energy starting event sample: Description and flux characterization with 7.5 years of data, IceCube Collaboration, Phys. Rev. D 104, 022002 (2021)

Tension between the Fermi diffuse gamma-ray sky and IceCube neutrino sky

Murase, Guetta, Ahlers (2016), Murase (2019)

- Calculation of the diffuse neutrino spectrum (with $\Gamma_\nu = 2.0$).
- Calculation of the corresponding diffuse gamma-ray spectrum, assuming sources are optically thin to two photon annihilation.
- To explain the <100 TeV IceCube neutrino observations (showers), *only* neutrino emitters should contribute to the Fermi isotropic diffuse gamma-ray background in the 3 GeV to 1 TeV range of the gamma-spectrum.
- Softer fluxes overshoot the data.



The flavor-averaged diffuse high-energy cosmic neutrino flux is related to cosmic-ray flux:

$$\frac{1}{3} \sum_{\alpha} E_{\nu}^2 \frac{dN_{\nu}}{dE_{\nu}} \simeq \frac{c}{4\pi} \left(\frac{1}{2} (1 - e^{-\tau_{p\gamma}}) \xi_z t_H \frac{dE}{dt} \right)$$

The IceCube all-flavor diffuse neutrino flux: $\sim 3 \times 10^{-11} \text{ TeV cm}^{-2} \text{ s}^{-1} \text{ sr}^{-1}$

The injection rate of cosmic rays above 10^{16} eV : $dE/dt \sim 1\text{-}2 \times 10^{44} \text{ erg Mpc}^{-3} \text{ yr}^{-1}$

Lead to optical depth for $p\gamma$ interactions as: $\tau_{p\gamma} \sim 0.4$

(assuming that muon neutrino emission rate follows a power law $E^{-\Gamma}$, where $\Gamma=2.19$)

$$\tau_{\gamma\gamma} \approx \frac{\eta_{\gamma\gamma} \sigma_{\gamma\gamma}}{\eta_{p\gamma} \hat{\sigma}_{p\gamma}} \tau_{p\gamma} \longrightarrow \tau_{\gamma\gamma} \sim \mathcal{O}(100)$$

The flavor-averaged diffuse high-energy cosmic neutrino flux is related to cosmic-ray flux:

$$\frac{1}{3} \sum_{\alpha} E_{\nu}^2 \frac{dN_{\nu}}{dE_{\nu}} \simeq \frac{c}{4\pi} \left(\frac{1}{2} (1 - e^{-\tau_{p\gamma}}) \xi_z t_H \frac{dE}{dt} \right)$$

The IceCube all-flavor diffuse neutrino flux: $\sim 3 \times 10^{-11} \text{ TeV cm}^{-2} \text{ s}^{-1} \text{ sr}^{-1}$

Theory suggests a gamma-ray flare is not expected when the source is a highly efficient neutrino emitter, since the gamma-gamma opacity is about 2 orders of magnitude larger than the gamma-proton opacity, that can explain the CR and neutrino observations.

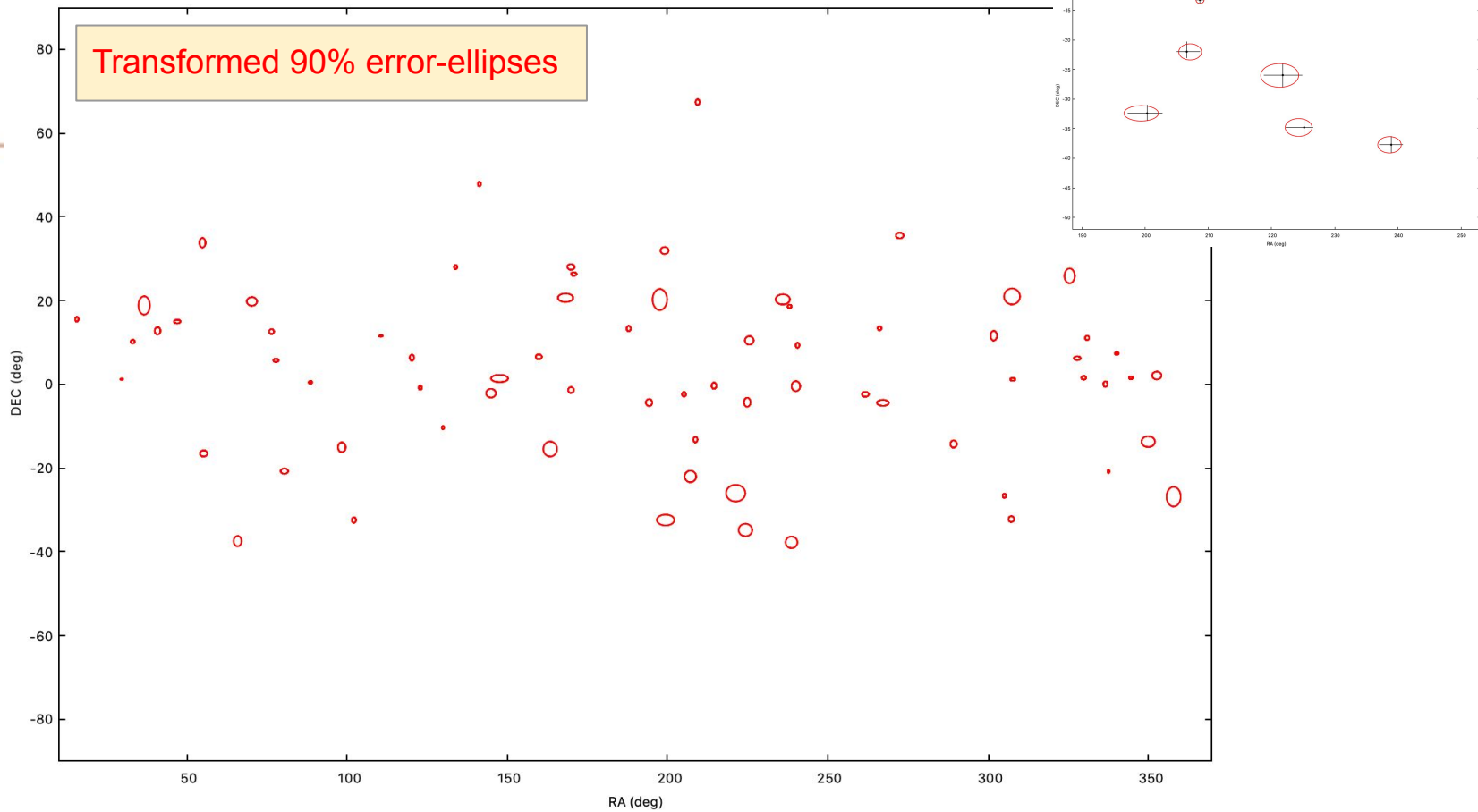
(e.g. Murase (2019), Halzen (2020))

(assuming that muon neutrino emission rate follows a power law $E^{-\Gamma}$, where $\Gamma = 2.15$)

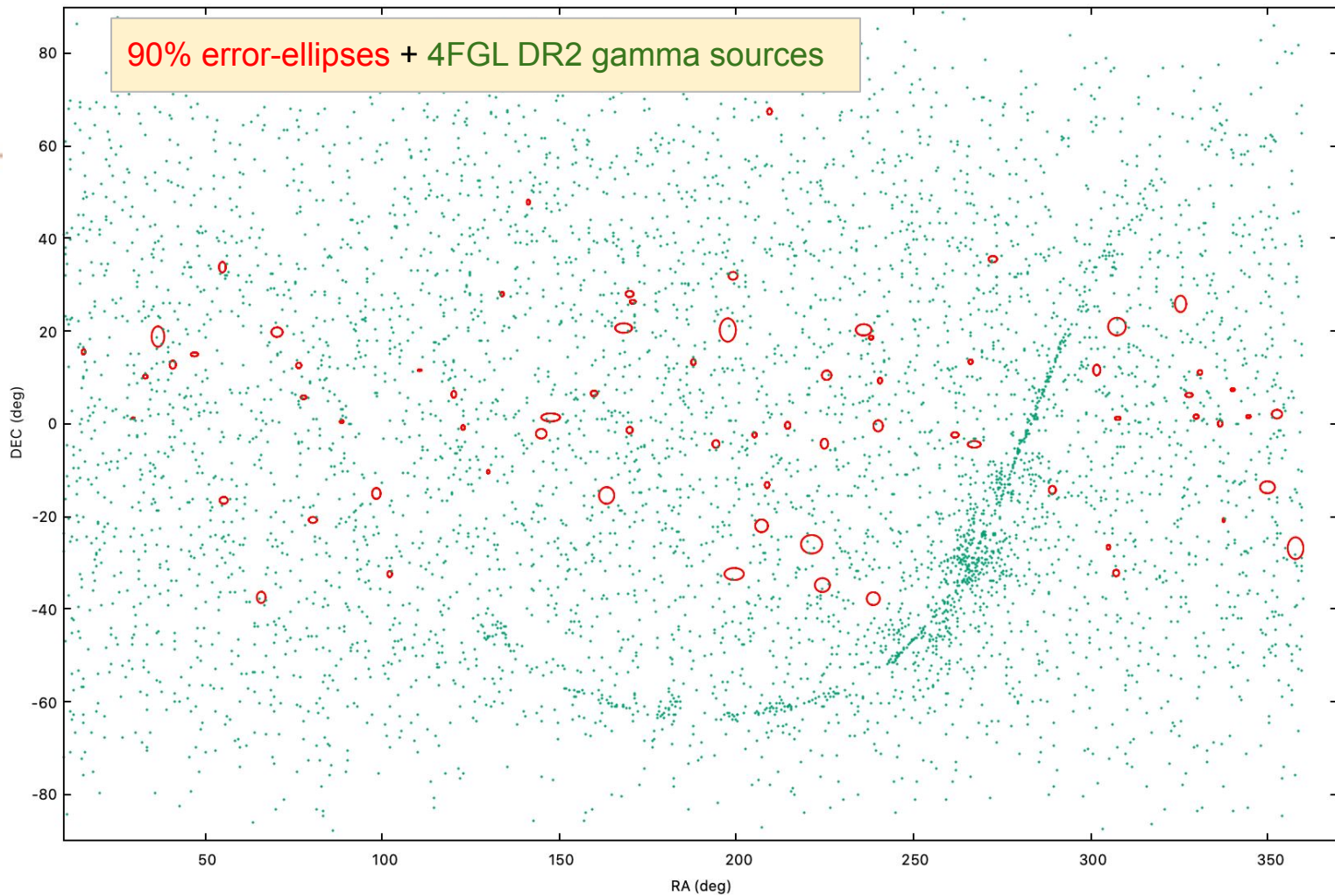
$$\tau_{\gamma\gamma} \approx \frac{\eta_{\gamma\gamma} \sigma_{\gamma\gamma}}{\eta_{p\gamma} \hat{\sigma}_{p\gamma}} \tau_{p\gamma} \longrightarrow \tau_{\gamma\gamma} \sim \mathcal{O}(100)$$

Likelihood analysis of 9 Fermi point sources within 90% containment area of track-type neutrino events published by Giommi et al. (2020)

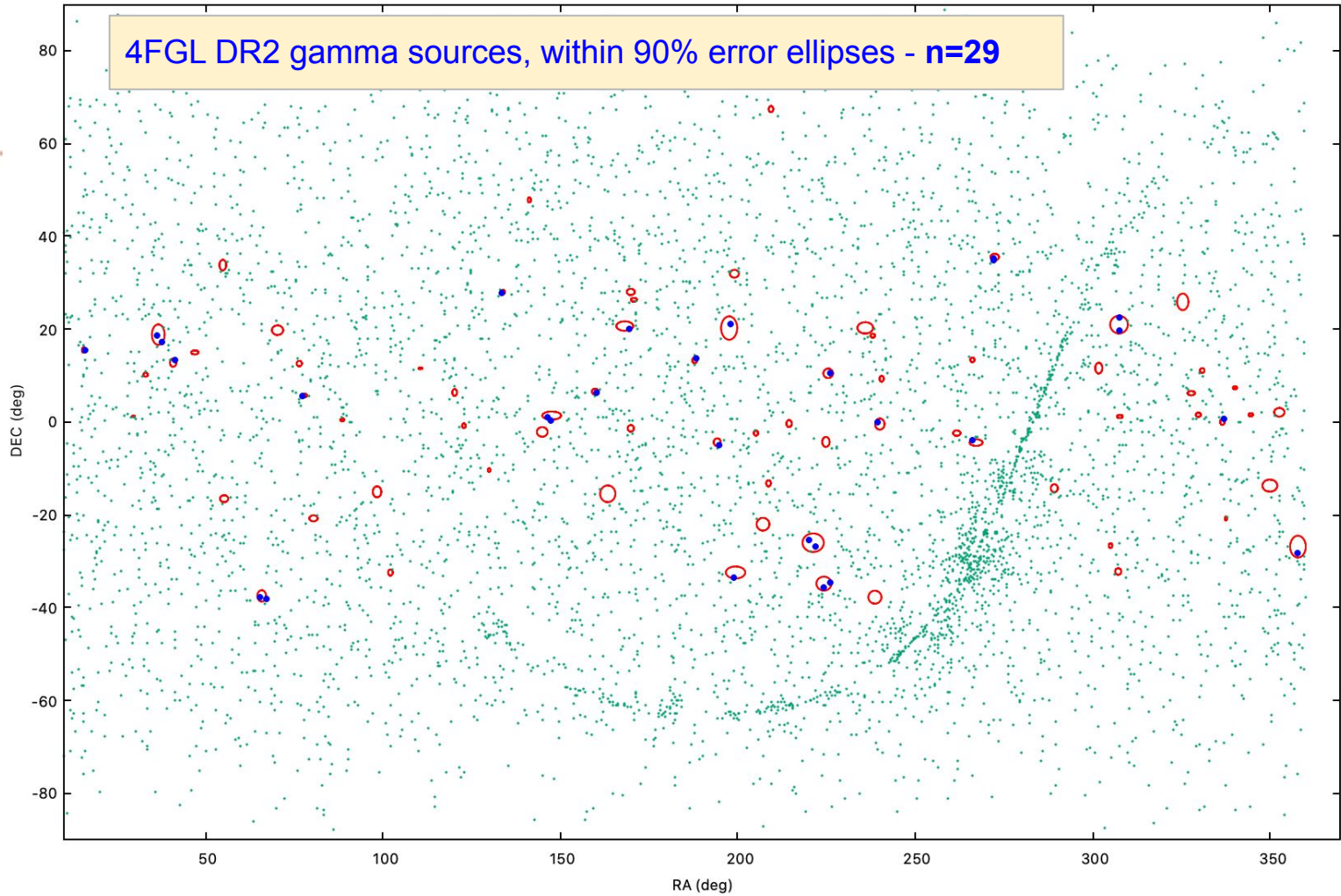
- Matched positions of point sources in the Fermi 4FGL DR2 catalog with track-type neutrinos from Giommi et al. (2020)
- Found 29 4FGL DR2 point sources, from which in case of 9 sources the predicted number of gamma-photons in 10 years is more than 1000 (5 BLL, 3 FSRQ, 1 SEY1)
- Generated the likelihood light curve of these gamma sources
- We see **IF** these AGN emit the neutrinos, neutrinos do not like to come during gamma-flares (4 after gamma flare, 1 before gamma flare, 1 at gamma flare, 1 between two gamma flares, 2?)



First we transformed the asymmetric error regions of neutrinos into ellipse shapes



4FGL DR2 gamma sources, within 90% error ellipses - n=29



Likelihood analysis of 9 Fermi point sources within 90% containment area of track-type neutrino events published by Giommi et al. (2020)

- Matched positions of point sources in the Fermi 4FGL DR2 catalog with track-type neutrinos from Giommi et al. (2020)
- Found 29 4FGL DR2 point sources, from which in case of 9 sources the predicted number of gamma-photons in 10 years is more than 1000 (5 BLL, 3 FSRQ, 1 SEY1)
- Generated the likelihood light curve of these gamma sources
- We see **IF** these AGN emit the neutrinos, neutrinos do not like to come during gamma-flares (4 after gamma flare, 1 before gamma flare, 1 at gamma flare, 1 between two gamma flares, 2?)

29 sources:

ID_ν	t_ν (MJD)	RA_ν ($^\circ$)	DEC_ν ($^\circ$)	ID_{4FGL}	RA_{4FGL} ($^\circ$)	DEC_{4FGL} ($^\circ$)
(1)	(2)	(3)	(4)	(5)	(6)	(7)
IC-100710A	55387.54	$307.53^{2.70}_{-2.28}$	$21.00^{2.25}_{-1.56}$	4FGL J2030.5+2235	307.63	22.59
IC-100710A	55387.54	$307.53^{2.70}_{-2.28}$	$21.00^{2.25}_{-1.56}$	4FGL J2030.9+1935	307.74	19.60
IC-110610A	55722.43	$272.49^{1.23}_{-1.19}$	$35.55^{0.69}_{-0.69}$	4FGL J1808.2+3500	272.07	35.01
IC-110610A	55722.43	$272.49^{1.23}_{-1.19}$	$35.55^{0.69}_{-0.69}$	4FGL J1808.8+3522	272.22	35.38
IC-110930A	55834.45	$267.23^{2.09}_{-1.55}$	$-4.41^{0.59}_{-0.86}$	4FGL J1744.2-0353	266.05	-3.89
IC-111216A	55911.28	$36.65^{1.85}_{-1.71}$	$18.85^{2.21}_{-2.21}$	4FGL J0230.3+1713	37.60	17.22
IC-111216A	55911.28	$36.65^{1.85}_{-1.71}$	$18.85^{2.21}_{-2.21}$	4FGL J0224.9+1843	36.23	18.72
IC-130408A	56390.19	$168.16^{2.87}_{-1.90}$	$20.67^{1.15}_{-0.89}$	4FGL J1117.0+2013	169.27	20.23
IC-140114A	56671.88	$336.71^{0.65}_{-0.65}$	$0.04^{0.65}_{-0.65}$	4FGL J2227.9+0036	336.98	0.62
IC-141126A	56987.77	$187.90^{0.65}_{-0.65}$	$13.30^{0.65}_{-0.65}$	4FGL J1233.0+1333	188.26	13.56
IC-141209A	57000.14	$159.81^{0.84}_{-1.04}$	$6.57^{0.64}_{-0.56}$	4FGL J1040.5+0617	160.15	6.28
IC-150904A	57269.80	$133.91^{0.39}_{-0.58}$	$28.00^{0.47}_{-0.47}$	4FGL J0854.0+2753	133.52	27.88
IC-150911A	57276.57	$240.09^{1.29}_{-1.38}$	$-0.45^{1.17}_{-1.23}$	4FGL J1557.9-0001	239.49	0.02
IC-150926A	57291.90	$194.25^{0.76}_{-1.21}$	$-4.34^{0.70}_{-0.95}$	4FGL J1258.7-0452	194.68	-4.87
IC-151017A	57312.70	$197.60^{2.46}_{-2.09}$	$20.26^{2.82}_{-2.21}$	4FGL J1311.8+2057	197.97	20.96
IC-160331A	57478.60	$15.60^{0.45}_{-0.58}$	$15.53^{0.53}_{-0.60}$	4FGL J0103.5+1526	15.88	15.43
IC-160814A	57614.91	$199.39^{2.43}_{-3.03}$	$-32.40^{1.39}_{-1.21}$	4FGL J1316.1-3338	199.03	-33.64
IC-161103A	57695.38	$40.83^{1.10}_{-0.70}$	$12.79^{1.10}_{-0.65}$	4FGL J0244.7+1316	41.19	13.28
IC-170506A	57879.53	$221.30^{3.00}_{-3.00}$	$-26.00^{2.00}_{-2.00}$	4FGL J1447.0-2657	221.76	-26.96
IC-170506A	57879.53	$221.30^{3.00}_{-3.00}$	$-26.00^{2.00}_{-2.00}$	4FGL J1439.5-2525	219.88	-25.42
IC-170922A	58018.87	$77.76^{0.95}_{-0.65}$	$5.72^{0.50}_{-0.30}$	4FGL J0509.4+0542	77.36	5.70
IC-181014A	58405.50	$224.30^{1.40}_{-2.85}$	$-34.80^{1.15}_{-1.85}$	4FGL J1457.4-3539	224.37	-35.65
IC-181014A	58405.50	$224.30^{1.40}_{-2.85}$	$-34.80^{1.15}_{-1.85}$	4FGL J1505.0-3433	226.26	-34.55
IC-190104A	58487.36	$357.98^{2.30}_{-2.10}$	$-26.85^{2.20}_{-2.50}$	4FGL J2351.4-2818	357.87	-28.31
IC-190504A	58607.77	$65.79^{1.23}_{-1.23}$	$-37.44^{1.23}_{-1.23}$	4FGL J0420.3-3745	65.09	-37.75
IC-190504A	58607.77	$65.79^{1.23}_{-1.23}$	$-37.44^{1.23}_{-1.23}$	4FGL J0428.6-3756	67.17	-37.94
IC-190730A	58694.87	$225.52^{1.28}_{-1.43}$	$10.47^{1.14}_{-0.89}$	4FGL J1504.4+1029	226.10	10.50
IC-190819A	58714.73	$147.56^{2.07}_{-3.24}$	$1.38^{1.00}_{-0.75}$	4FGL J0946.2+0104	146.57	1.07
IC-190819A	58714.73	$147.56^{2.07}_{-3.24}$	$1.38^{1.00}_{-0.75}$	4FGL J0948.9+0022	147.24	0.37

Table 4: Neutrino source candidates from 10 year Fermi Point Source Catalogue (4FGL DR2) ($n = 29$, out of 5712). Neutrino ID (1), detection time (2), arrival direction of neutrino (90% containment, 3-4), 4FGL source (5), its position (6-7).

Kun et al., in prep.

Source (1)	RA (2)	DEC (3)	Npred (4)	Flux1000 (5)	FluxPeak (6)	CLASS1 (7)	ASSOC1 (8)
4FGL J2030.5+2235	307.64	22.59	117.0	1.36e-10	nan		
4FGL J2030.9+1935	307.74	19.60	526.8	8.24e-10	nan	BLL	RX J2030.8+1935
4FGL J1808.2+3500	272.07	35.01	730.8	3.72e-10	1.75e-08	BLL	MG2 J180813+3501
4FGL J1808.8+3522	272.22	35.38	305.6	1.91e-10	nan	BLL	2MASX J18084968+3520426
4FGL J1744.2-0353	266.05	-3.89	740.6	3.90e-10	nan	FSRQ	PKS 1741-03
4FGL J0230.3+1713	37.60	17.22	537.5	2.52e-10	nan		
4FGL J0224.9+1843	36.23	18.72	983.7	1.70e-10	4.52e-08	FSRQ	TXS 0222+185
4FGL J1117.0+2013	169.27	20.23	1442.3	1.25e-09	2.09e-08	BLL	RBS 0958
4FGL J2227.9+0036	336.98	0.62	679.9	8.70e-10	nan	BLL	PMN J2227+0037
4FGL J1233.0+1333	188.26	13.56	828.0	3.34e-10	nan		
4FGL J1040.5+0617	160.15	6.28	2927.1	1.49e-09	6.26e-08	BLL	GB6 J1040+0617
4FGL J0854.0+2753	133.52	27.88	28.4	3.93e-11	nan	BLL	SDSS J085410.16+275421.7
4FGL J1557.9-0001	239.49	-0.02	412.3	1.86e-10	nan	FSRQ	PKS 1555+001
4FGL J1258.7-0452	194.68	-4.87	124.1	1.73e-10	nan	BLL	RBS 1194
4FGL J1311.8+2057	197.97	20.96	617.2	5.30e-11	nan	bcu	MG2 J131144+2052
4FGL J0103.5+1526	15.88	15.43	294.7	1.74e-10	nan	BLL	TXS 0100+151
4FGL J1316.1-3338	199.03	-33.64	3866.4	2.39e-09	1.22e-07	FSRQ	PKS 1313-333
4FGL J0244.7+1316	41.19	13.28	574.5	2.01e-10	1.78e-08	Blazar	GB6 J0244+1320
4FGL J1447.0-2657	221.77	-26.96	195.1	1.64e-10	nan	bcu	NVSS J144657-265713
4FGL J1439.5-2525	219.88	-25.42	153.9	1.55e-10	nan	bcu	NVSS J143934-252458
4FGL J0509.4+0542	77.36	5.70	7619.8	8.02e-09	1.94e-07	BLL	TXS 0506+056
4FGL J1457.4-3539	224.37	-35.65	5233.2	3.49e-09	2.56e-07	FSRQ	PKS 1454-354
4FGL J1505.0-3433	226.26	-34.55	642.8	3.77e-10	2.15e-08	BLL	PMN J1505-3432
4FGL J2351.4-2818	357.87	-28.31	290.7	1.28e-10	nan		
4FGL J0420.3-3745	65.09	-37.75	1841.0	1.09e-09	3.43e-08	BLL*	NVSS J042025-374443
4FGL J0428.6-3756	67.17	-37.94	24240.385	2.36e-08	3.57e-07	BLL	PKS 0426-380 [∘]
4FGL J1504.4+1029	226.10	10.50	25352.5	2.02e-08	9.72e-07	FSRQ	PKS 1502+106
4FGL J0946.2+0104	146.57	1.07	201.8	2.15e-10	nan	BLL	1RXS J094620.5+010459
4FGL J0948.9+0022	147.24	0.37	7769.2	2.29e-09	1.61e-07	NLSY1	PMN J0948+0022

Table 7: Source properties from 4FGL DR2 (10 years Fermi point source catalog). (1) 4FGL source name. (2) RAJ2000. (3) DECJ2000. (4) Npred=predicted number of photons. (5) Flux1000: flux between 0.1-100 GeV ($ph/cm^2/s$). (6) Flux peak ($ph/cm^2/s$). (7) Types: bcu = active galaxy of uncertain type,fsrq = FSRQ type of blazar,bll = BL Lac type of blazar; *: object type according to Simbad. (8) Association name. [∘]: within 90% neutrino containment area (GCN CIRCULAR 24401).

Source properties
from 4FGL DR2:

Kun et al., in prep.

Source (1)	RA (2)	DEC (3)	Npred (4)	Flux1000 (5)	FluxPeak (6)	CLASS1 (7)	ASSOC1 (8)
4FGL J2030.5+2235	307.64	22.59	117.0	1.36e-10	nan		
4FGL J2030.9+1935	307.74	19.60	526.8	8.24e-10	nan	BLL	RX J2030.8+1935
4FGL J1808.2+3500	272.07	35.01	730.8	3.72e-10	1.75e-08	BLL	MG2 J180813+3501
4FGL J1808.8+3522	272.22	35.38	305.6	1.91e-10	nan	BLL	2MASX J18084968+3520426
4FGL J1744.2-0353	266.05	-3.89	740.6	3.90e-10	nan	FSRQ	PKS 1741-03
4FGL J0230.3+1713	37.60	17.22	537.5	2.52e-10	nan		
4FGL J0224.9+1843	36.23	18.72	983.7	1.70e-10	4.52e-08	FSRQ	TXS 0222+185
4FGL J1117.0+2013	169.27	20.23	1442.3	1.25e-09	2.09e-08	BLL	RBS 0958
4FGL J2227.9+0036	336.98	0.62	679.9	8.70e-10	nan	BLL	PMN J2227+0037
4FGL J1233.0+1333	188.26	13.56	828.0	3.34e-10	nan		
4FGL J1040.5+0617	160.15	6.28	2927.1	1.49e-09	6.26e-08	BLL	GB6 J1040+0617
4FGL J0854.0+2753	133.52	27.88	28.4	3.93e-11	nan	BLL	SDSS J085410.16+275421.7
4FGL J1557.9-0001	239.49	-0.02	412.3	1.86e-10	nan	FSRQ	PKS 1555+001
4FGL J1258.7-0452	194.68	-4.87	124.1	1.73e-10	nan	BLL	RBS 1194
4FGL J1311.8+2057	197.97	20.96	617.2	5.30e-11	nan	bcu	MG2 J131144+2052
4FGL J0103.5+1526	15.88	15.43	294.7	1.74e-10	nan	BLL	TXS 0100+151
4FGL J1316.1-3338	199.03	-33.64	3866.4	2.39e-09	1.22e-07	FSRQ	PKS 1313-333
4FGL J0244.7+1316	41.19	13.28	574.5	2.01e-10	1.78e-08	Blazar	GB6 J0244+1320
4FGL J1447.0-2657	221.77	-26.96	195.1	1.64e-10	nan	bcu	NVSS J144657-265713
4FGL J1439.5-2525	219.88	-25.42	153.9	1.55e-10	nan	bcu	NVSS J143934-252458
4FGL J0509.4+0542	77.36	5.70	7619.8	8.02e-09	1.94e-07	BLL	TXS 0506+056
4FGL J1457.4-3539	224.37	-35.65	5233.2	3.49e-09	2.56e-07	FSRQ	PKS 1454-354
4FGL J1505.0-3433	226.26	-34.55	642.8	3.77e-10	2.15e-08	BLL	PMN J1505-3432
4FGL J2351.4-2818	357.87	-28.31	290.7	1.28e-10	nan		
4FGL J0420.3-3745	65.09	-37.75	1841.0	1.09e-09	3.43e-08	BLL*	NVSS J042025-374443
4FGL J0428.6-3756	67.17	-37.94	24240.385	2.36e-08	3.57e-07	BLL	PKS 0426-380 [∘]
4FGL J1504.4+1029	226.10	10.50	25352.5	2.02e-08	9.72e-07	FSRQ	PKS 1502+106
4FGL J0946.2+0104	146.57	1.07	201.8	2.15e-10	nan	BLL	1RXS J094620.5+010459
4FGL J0948.9+0022	147.24	0.37	7769.2	2.29e-09	1.61e-07	NLSY1	PMN J0948+0022

Table 7: Source properties from 4FGL DR2 (10 years Fermi point source catalog). (1) 4FGL source name. (2) RAJ2000. (3) DECJ2000. (4) Npred=predicted number of photons. (5) Flux1000: flux between 0.1-100 GeV ($ph/cm^2/s$). (6) Flux peak ($ph/cm^2/s$). (7) Types: bcu = active galaxy of uncertain type,fsrq = FSRQ type of blazar,bll = BL Lac type of blazar; *: object type according to Simbad. (8) Association name. [∘]: within 90% neutrino containment area (GCN CIRCULAR 24401).

Source properties
from 4FGL DR2:

Kun et al., in prep.

Let's focus on the gamma regime (4FGL DR2)

We picked gamma sources with NPred > 1000 (predicted number of gamma photons), otherwise too dim to be analysed - 9 gamma sources remain in the sample (out of 29)

Source (1)	RA (2)	DEC (3)	Npred (4)	Flux1000 (5)	FluxPeak (6)	CLASS1 (7)	ASSOC1 (8)
4FGL J1117.0+2013	169.27	20.23	1442.3	1.25e-09	2.09e-08	BLL	RBS 0958
4FGL J1040.5+0617	160.15	6.28	2927.1	1.49e-09	6.26e-08	BLL	GB6 J1040+0617
4FGL J1316.1-3338	199.03	-33.64	3866.4	2.39e-09	1.22e-07	FSRQ	PKS 1313-333
4FGL J0509.4+0542	77.36	5.70	7619.8	8.02e-09	1.94e-07	BLL	TXS 0506+056
4FGL J1457.4-3539	224.37	-35.65	5233.2	3.49e-09	2.56e-07	FSRQ	PKS 1454-354
4FGL J0420.3-3745	65.09	-37.75	1841.0	1.09e-09	3.43e-08	BLL*	NVSS J042025-374443
4FGL J0428.6-3756	67.17	-37.94	24240.385	2.36e-08	3.57e-07	BLL	PKS 0426-380 ^x
4FGL J1504.4+1029	226.10	10.50	25352.5	2.02e-08	9.72e-07	FSRQ	PKS 1502+106
4FGL J0948.9+0022	147.24	0.37	7769.2	2.29e-09	1.61e-07	NLSY1	PMN J0948+0022

Kun et al., in prep.

Downloaded Fermi data within +/- half year about the corresponding neutrinos

Likelihood analysis of 9 Fermi point sources within 90% containment area of track-type neutrino events published by Giommi et al. (2020)

- Matched positions of point sources in the Fermi 4FGL DR2 catalog with track-type neutrinos from Giommi et al. (2020)
- Found 29 4FGL DR2 point sources, from which in case of 9 sources the predicted number of gamma-photons in 10 years is more than 1000 (5 BLL, 3 FSRQ, 1 SEY1)
- **Generated the likelihood light curve of these gamma sources**
- We see **IF** these AGN emit the neutrinos, neutrinos do not like to come during gamma-flares (4 after gamma flare, 1 before gamma flare, 1 at gamma flare, 1 between two gamma flares, 2?)

Likelihood analysis of 9 Fermi point sources within 90% containment area of track-type neutrino events published by Giommi et al. (2020)

Technical information:

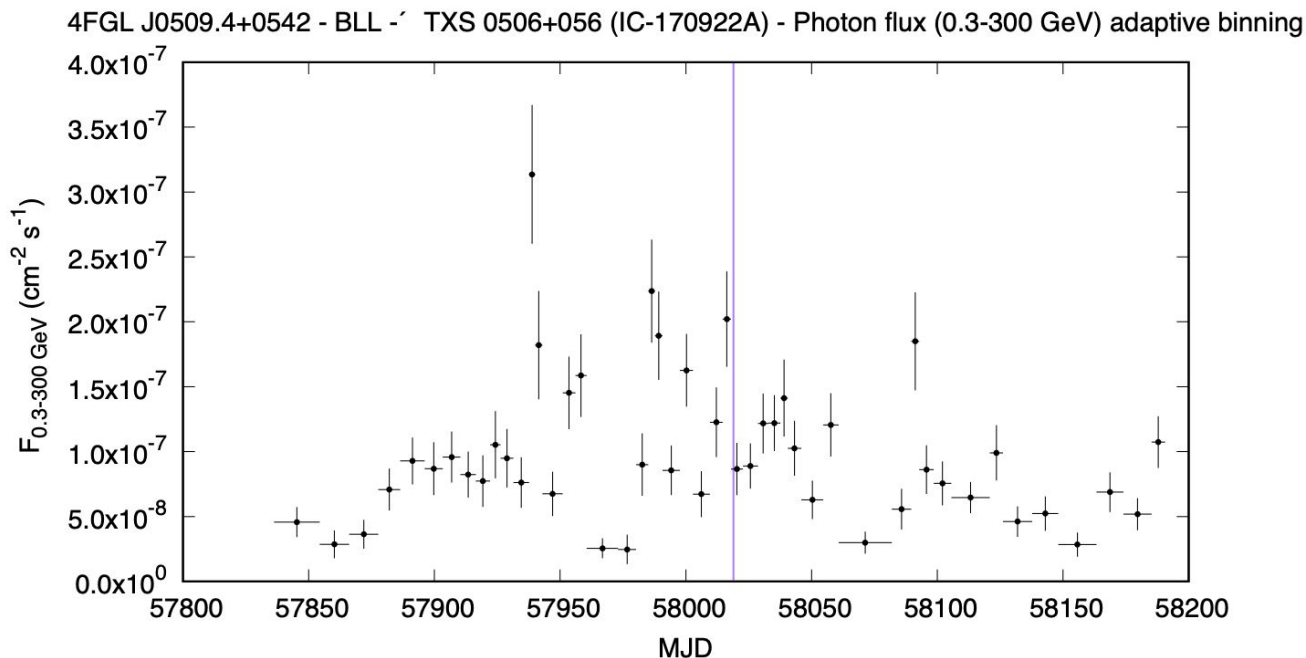
- Dedicated project on a cluster of 16x2.2 GHz Intel Skylake vCPUs (PI: EK), ELKH Cloud (Hungary, Wigner Data Center), using Docker technology

Software packages: fermipy v1.0.1, ScienceTools v2.0.8 (FermiBottle)

- Instrument response function: P8R3_SOURCE_V2_v1
- Galactic interstellar emission model: gll_iem_v07.fits
- Isotropic diffuse emission model: iso_P8R3_SOURCE_V2_v1.txt

- Standard quality cuts ($z_{\max}=90$, $(\text{DATA_QUAL} > 0) \ \&\&(\text{LAT_CONFIG}==1)$)
- Minimum separation between two new point sources: 0.3 deg, $\text{TS}_{\min}=25$ ($\sim 5\sigma$)
- Adaptive binning (Lott et al. 2012, 10%-15%-20%)

BLL



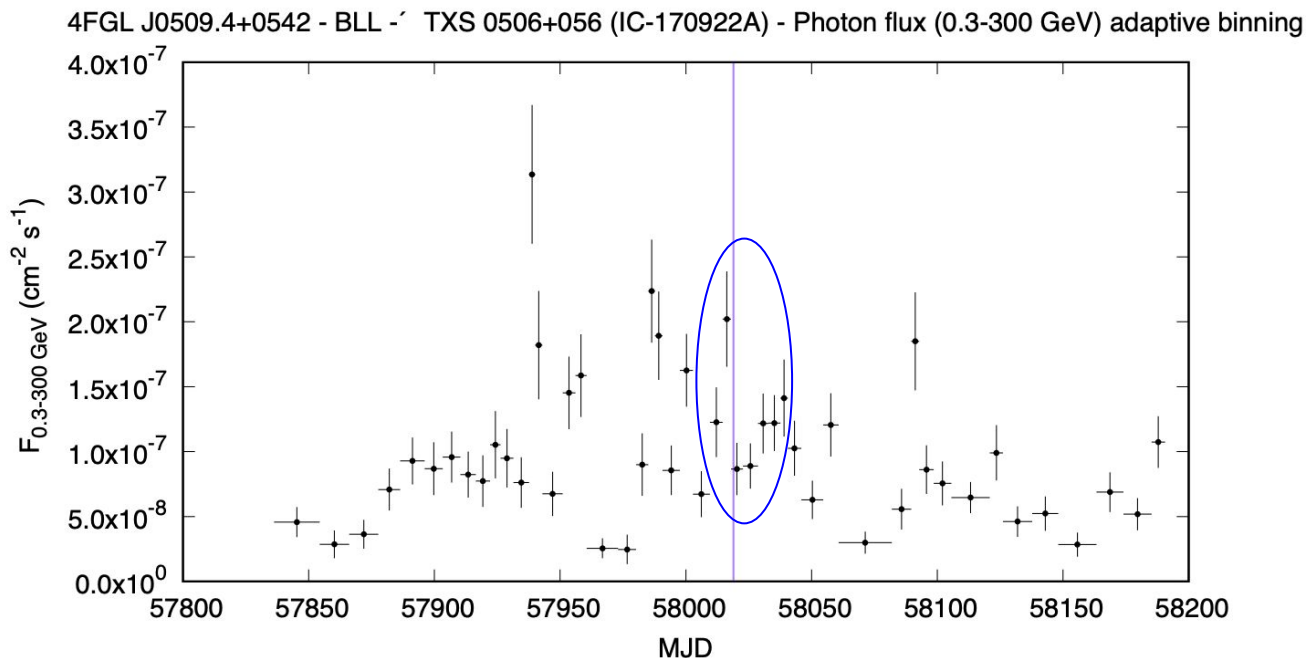
TS ≤ 9
 9 < TS ≤ 25
 TS > 25

Kun et al., in prep.

- $\text{TS} = -2\ln(L_{\text{max},0}/L_{\text{max},1})$, where $L_{\text{max},0}$ is the maximum likelihood value for a model without an additional source (the 'null hypothesis') and $L_{\text{max},1}$ is the maximum likelihood value for a model with the additional source at a specified location

- Basic rule of thumb, **the square root of the TS is approximately equal to the detection significance for a given source** 27

BLL



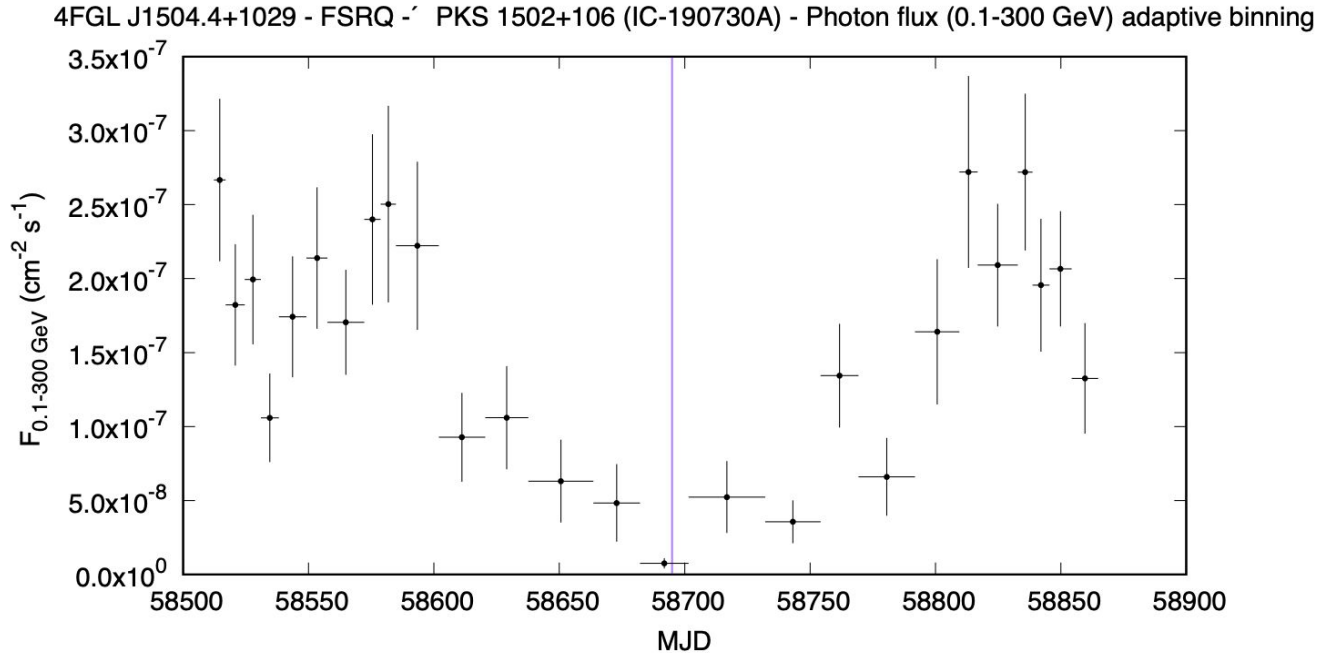
TS ≤ 9
 9 < TS ≤ 25
 TS > 25

Kun et al., in prep.

- $TS = -2 \ln(L_{max,0}/L_{max,1})$, where $L_{max,0}$ is the maximum likelihood value for a model without an additional source (the 'null hypothesis') and $L_{max,1}$ is the maximum likelihood value for a model with the additional source at a specified location

- Basic rule of thumb, **the square root of the TS is approximately equal to the detection significance for a given source** 28

FSRQ



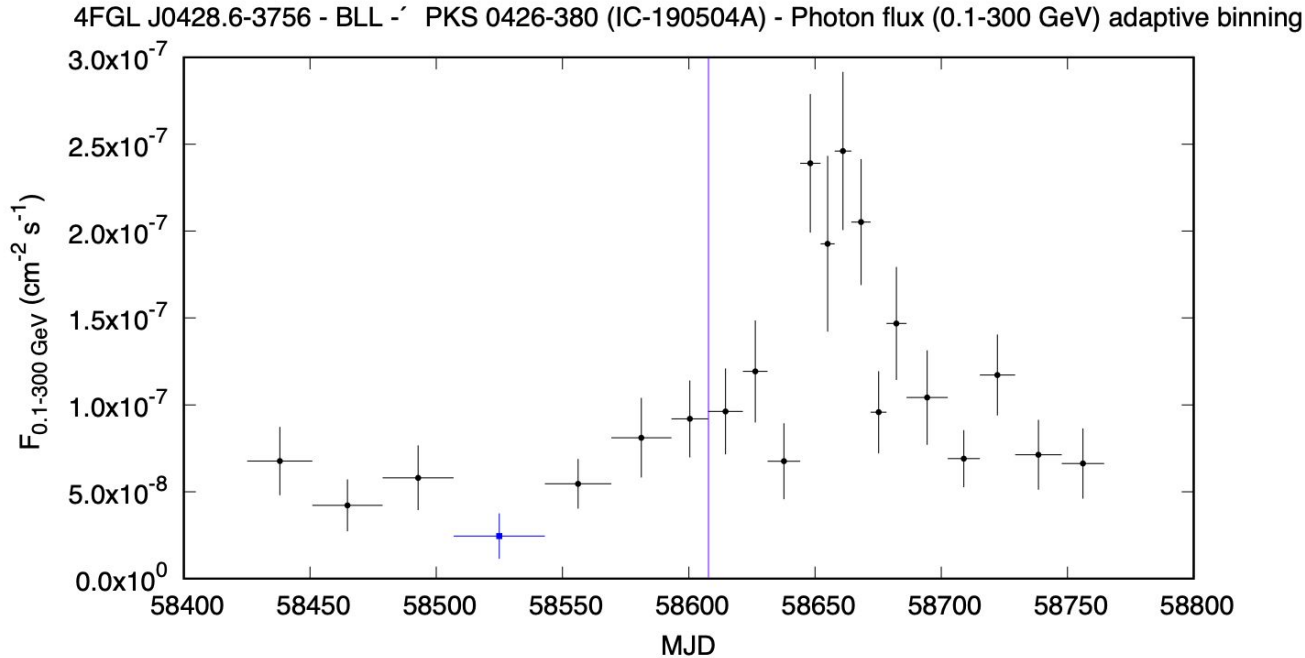
$TS \leq 9$
 $9 < TS \leq 25$
 $TS > 25$

Kun et al., in prep.

- $TS = -2 \ln(L_{max,0}/L_{max,1})$, where $L_{max,0}$ is the maximum likelihood value for a model without an additional source (the 'null hypothesis') and $L_{max,1}$ is the maximum likelihood value for a model with the additional source at a specified location

- Basic rule of thumb, **the square root of the TS is approximately equal to the detection significance for a given source** 29

BLL



TS ≤ 9
 9 < TS ≤ 25
 TS > 25

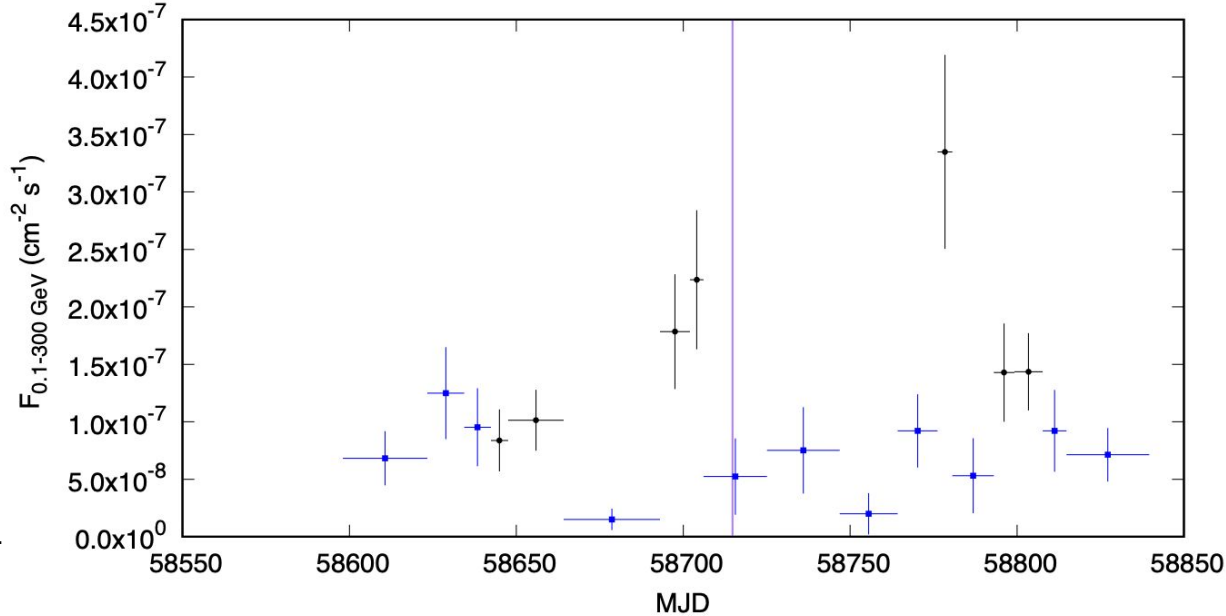
Kun et al., in prep.

- $TS = -2 \ln(L_{max,0} / L_{max,1})$, where $L_{max,0}$ is the maximum likelihood value for a model without an additional source (the 'null hypothesis') and $L_{max,1}$ is the maximum likelihood value for a model with the additional source at a specified location

- Basic rule of thumb, **the square root of the TS is approximately equal to the detection significance for a given source** 30

SEY1

4FGL J0948.9+0022 - NLSY1 - PMN J0948+0022 (IC-190819A) - Photon flux (0.1-300 GeV) adaptive binning



TS ≤ 9
 9 < TS ≤ 25
 TS > 25

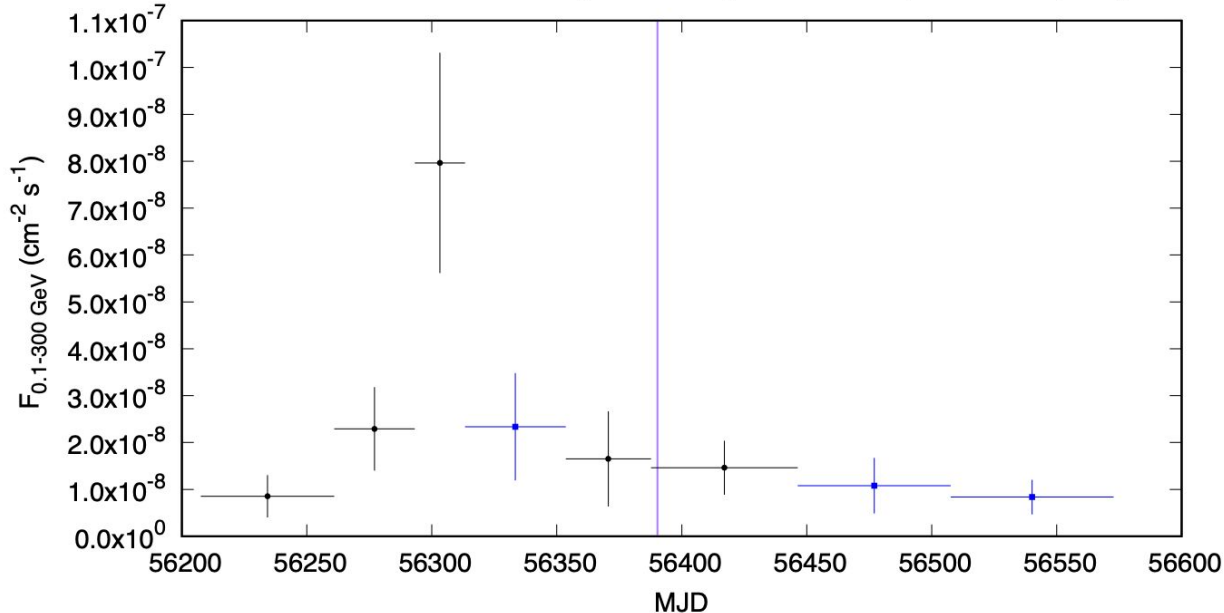
Kun et al., in prep.

- $TS = -2 \ln(L_{max,0} / L_{max,1})$, where $L_{max,0}$ is the maximum likelihood value for a model without an additional source (the 'null hypothesis') and $L_{max,1}$ is the maximum likelihood value for a model with the additional source at a specified location

- Basic rule of thumb, **the square root of the TS is approximately equal to the detection significance for a given source** 31

BLL

4FGL J1117.0+2013 - BLL - RBS 0958 (IC-130408A) - Photon flux (0.1-300 GeV) adaptive binning



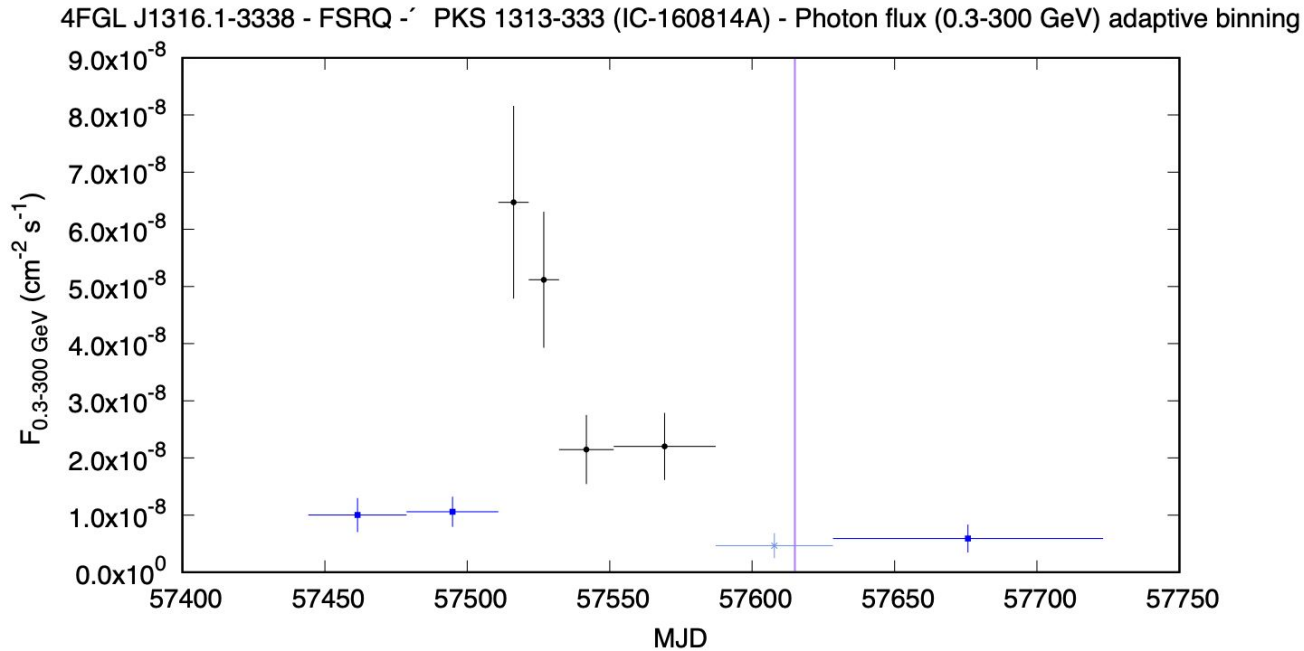
TS ≤ 9
 9 < TS ≤ 25
 TS > 25

Kun et al., in prep.

- $\text{TS} = -2 \ln(L_{\text{max},0} / L_{\text{max},1})$, where $L_{\text{max},0}$ is the maximum likelihood value for a model without an additional source (the 'null hypothesis') and $L_{\text{max},1}$ is the maximum likelihood value for a model with the additional source at a specified location

- Basic rule of thumb, **the square root of the TS is approximately equal to the detection significance for a given source** 32

FSRQ



TS ≤ 9
 9 < TS ≤ 25
 TS > 25

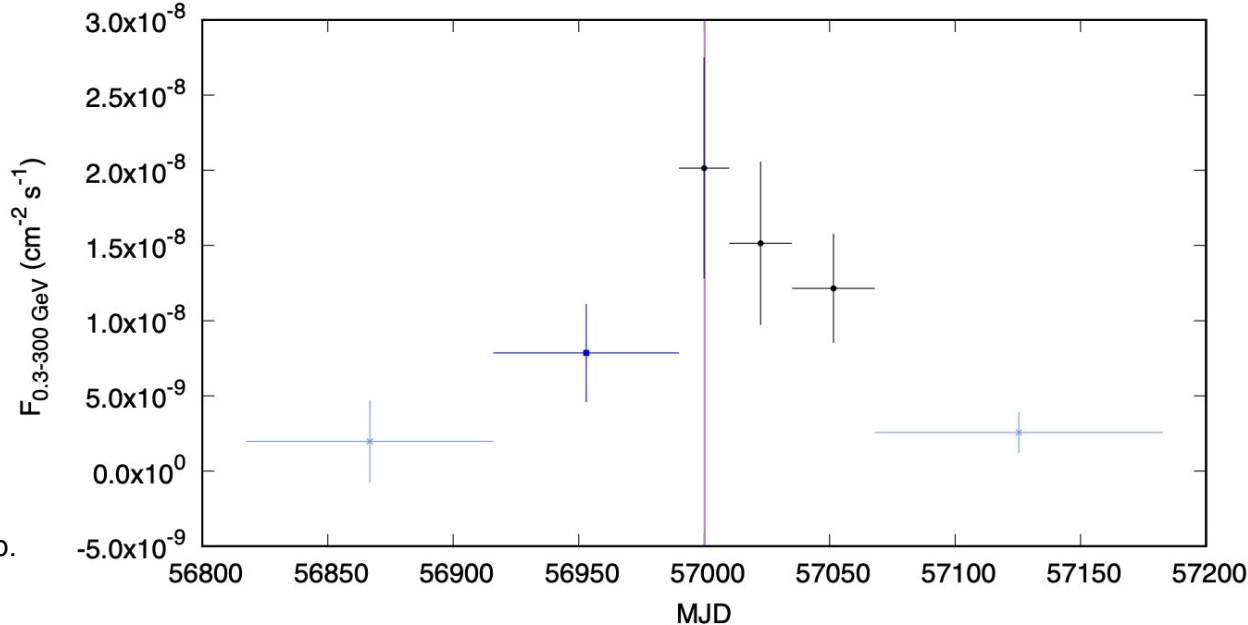
Kun et al., in prep.

- $\text{TS} = -2 \ln(L_{\text{max},0} / L_{\text{max},1})$, where $L_{\text{max},0}$ is the maximum likelihood value for a model without an additional source (the 'null hypothesis') and $L_{\text{max},1}$ is the maximum likelihood value for a model with the additional source at a specified location

- Basic rule of thumb, **the square root of the TS is approximately equal to the detection significance for a given source** 33

BLL

4FGL J1040.5+0617 - BLL - GB6 J1040+0617 (IC-141209A) - Photon flux (0.3-300 GeV) adaptive binning



TS ≤ 9
 9 < TS ≤ 25
 TS > 25

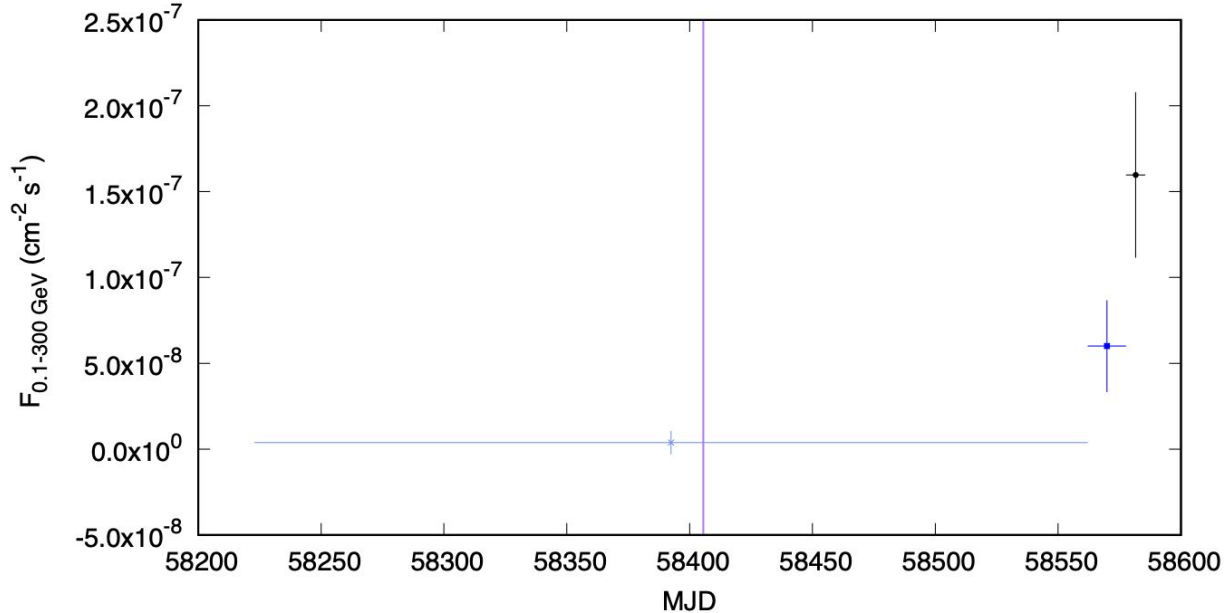
Kun et al., in prep.

- $\text{TS} = -2 \ln(L_{\text{max},0} / L_{\text{max},1})$, where $L_{\text{max},0}$ is the maximum likelihood value for a model without an additional source (the 'null hypothesis') and $L_{\text{max},1}$ is the maximum likelihood value for a model with the additional source at a specified location

- Basic rule of thumb, **the square root of the TS is approximately equal to the detection significance for a given source** 34

FSRQ

4FGL J1457.4-3539 - FSRQ - ' PKS 1454-354 (IC-181014A) - Photon flux (0.1-300 GeV) adaptive binning



TS ≤ 9
 9 < TS ≤ 25
 TS > 25

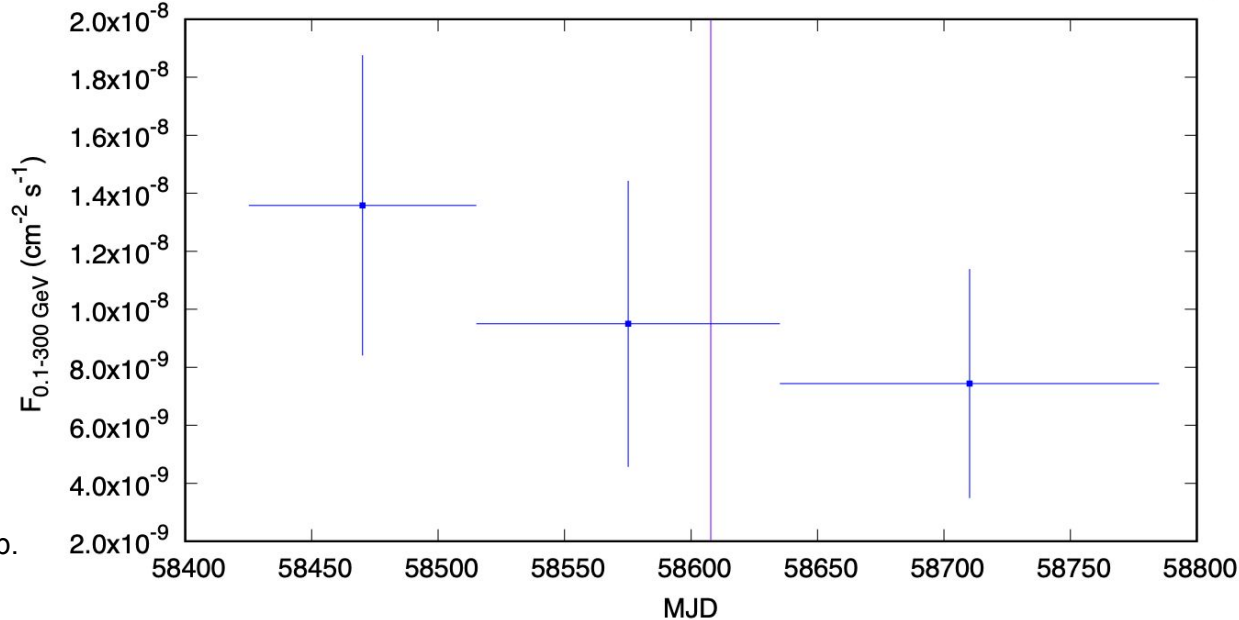
Kun et al., in prep.

- $TS = -2 \ln(L_{max,0} / L_{max,1})$, where $L_{max,0}$ is the maximum likelihood value for a model without an additional source (the 'null hypothesis') and $L_{max,1}$ is the maximum likelihood value for a model with the additional source at a specified location

- Basic rule of thumb, **the square root of the TS is approximately equal to the detection significance for a given source** 35

?

4FGL J0420.3-3745 - bcu - NVSS J042025-374443 (IC-190504A) - Photon flux (0.1-300 GeV) adaptive binning



TS ≤ 9
 9 < TS ≤ 25
 TS > 25

Kun et al., in prep.

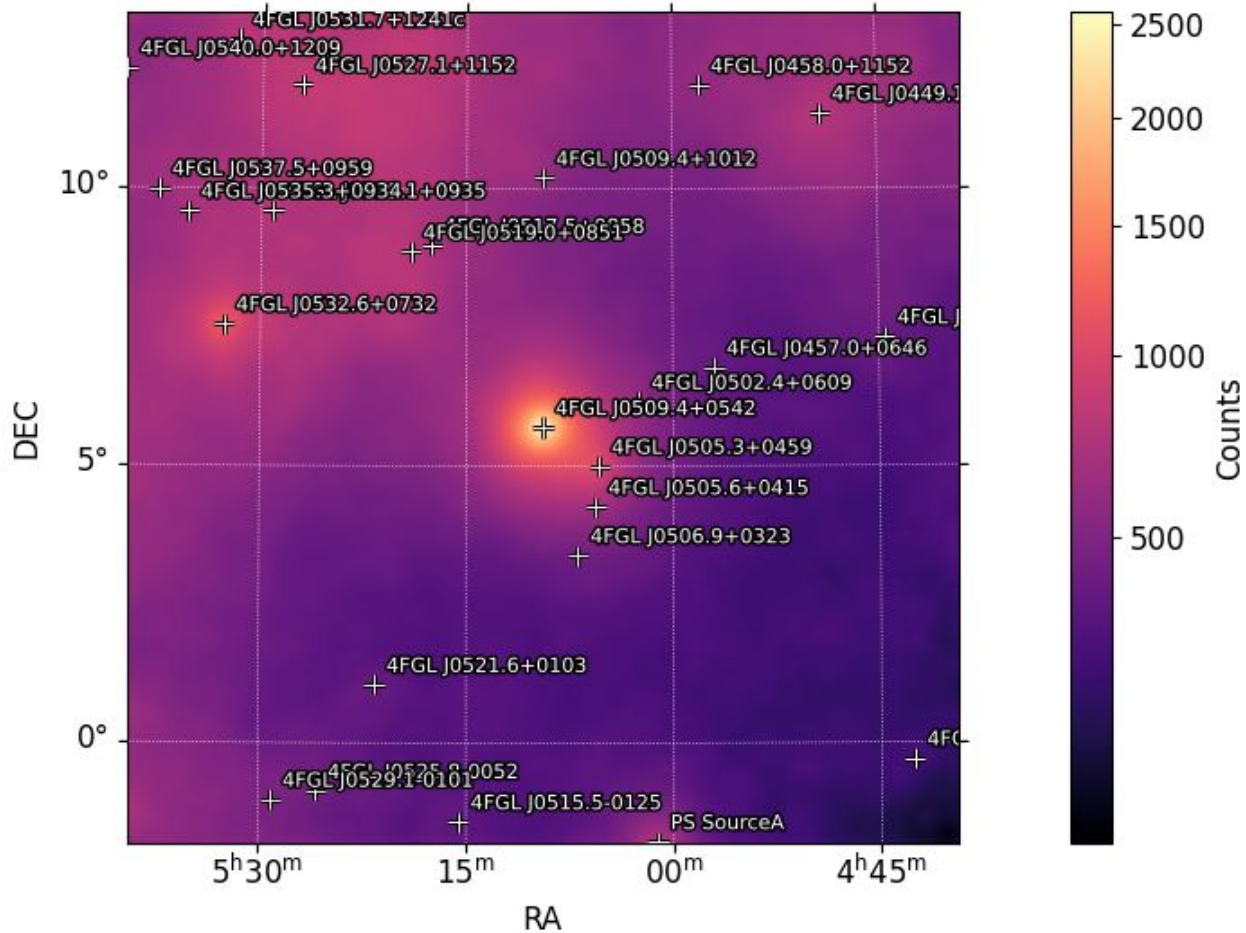
- $TS = -2 \ln(L_{max,0}/L_{max,1})$, where $L_{max,0}$ is the maximum likelihood value for a model without an additional source (the 'null hypothesis') and $L_{max,1}$ is the maximum likelihood value for a model with the additional source at a specified location

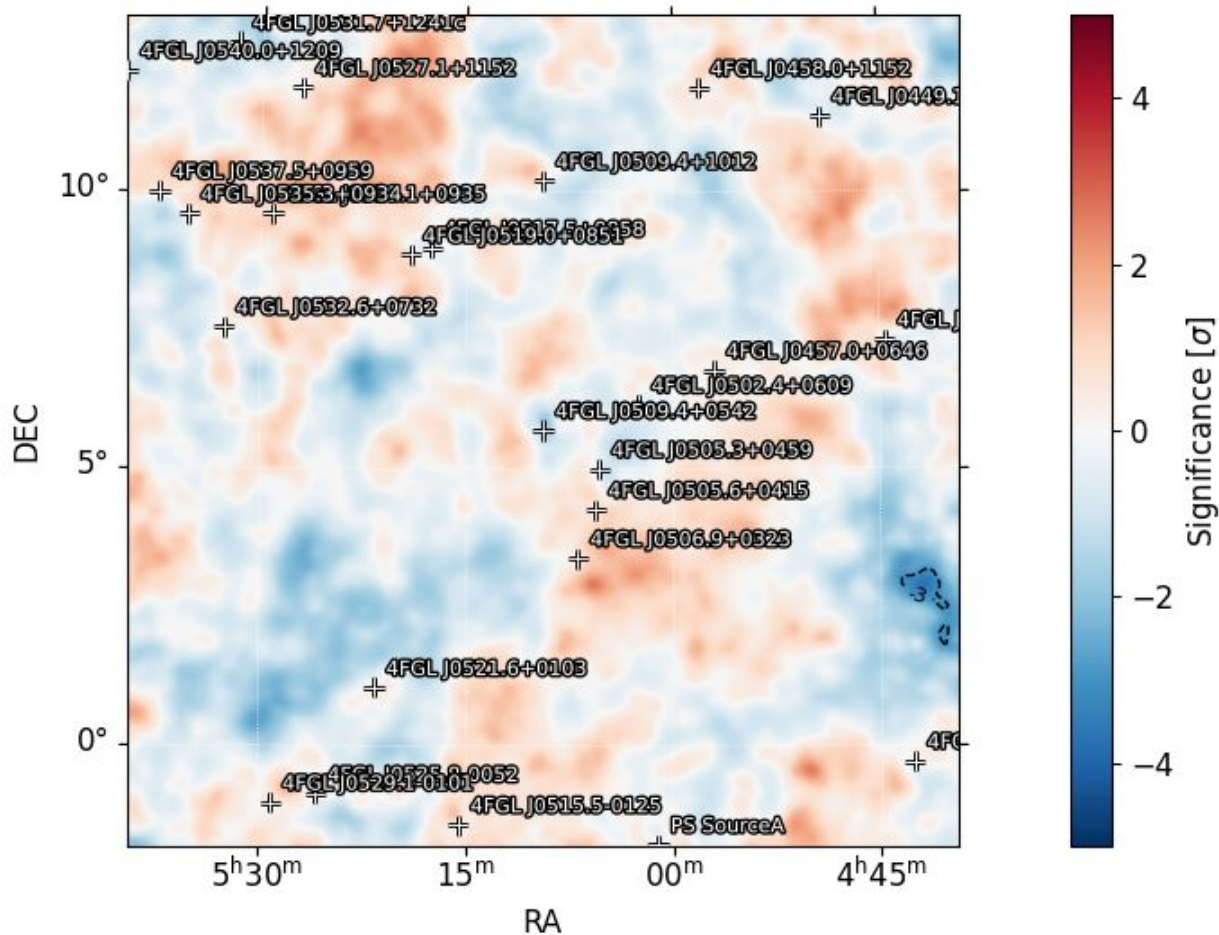
- Basic rule of thumb, **the square root of the TS is approximately equal to the detection significance for a given source** 36

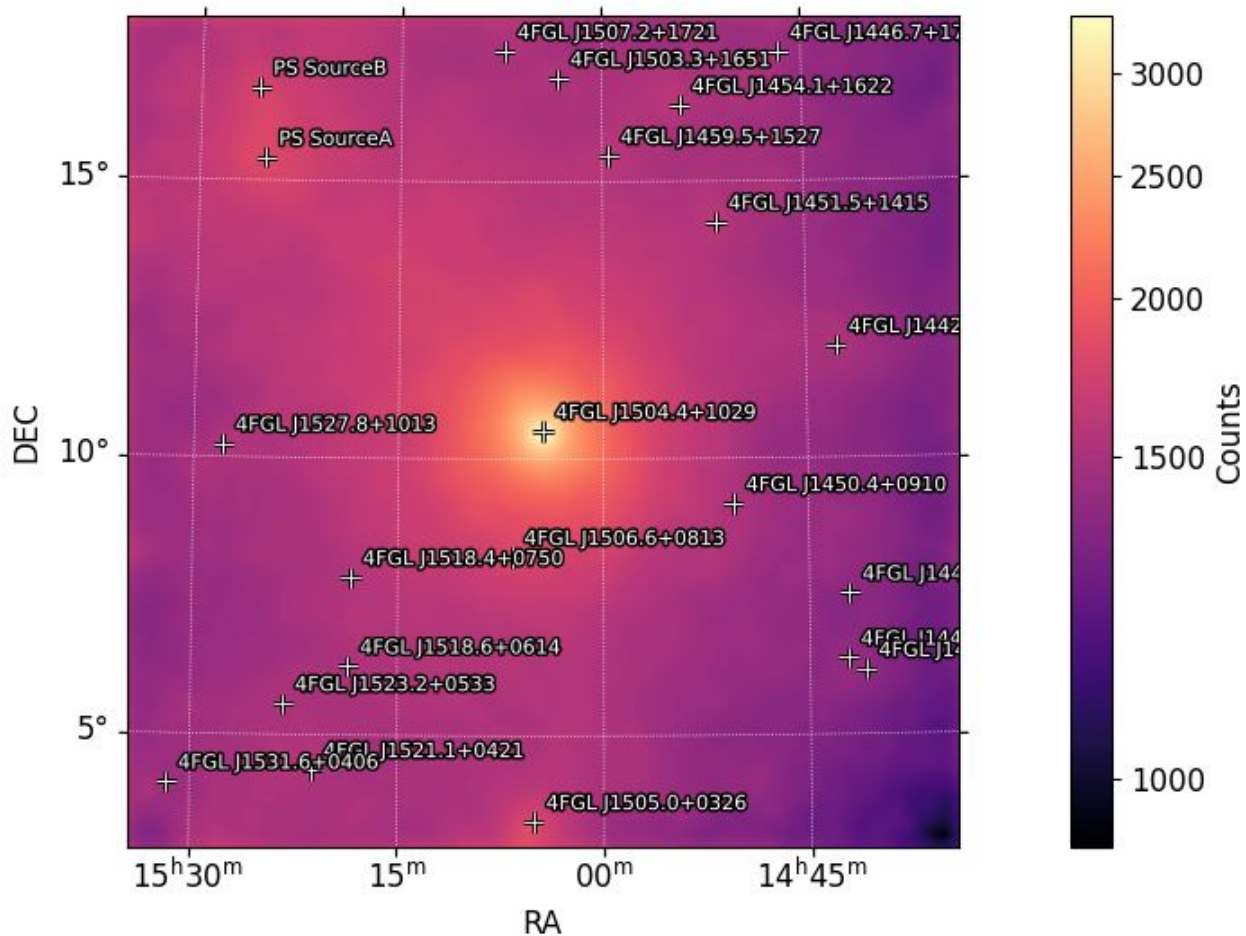
Likelihood analysis of 9 Fermi point sources within 90% containment area of track-type neutrino events published by Giommi et al. (2020)

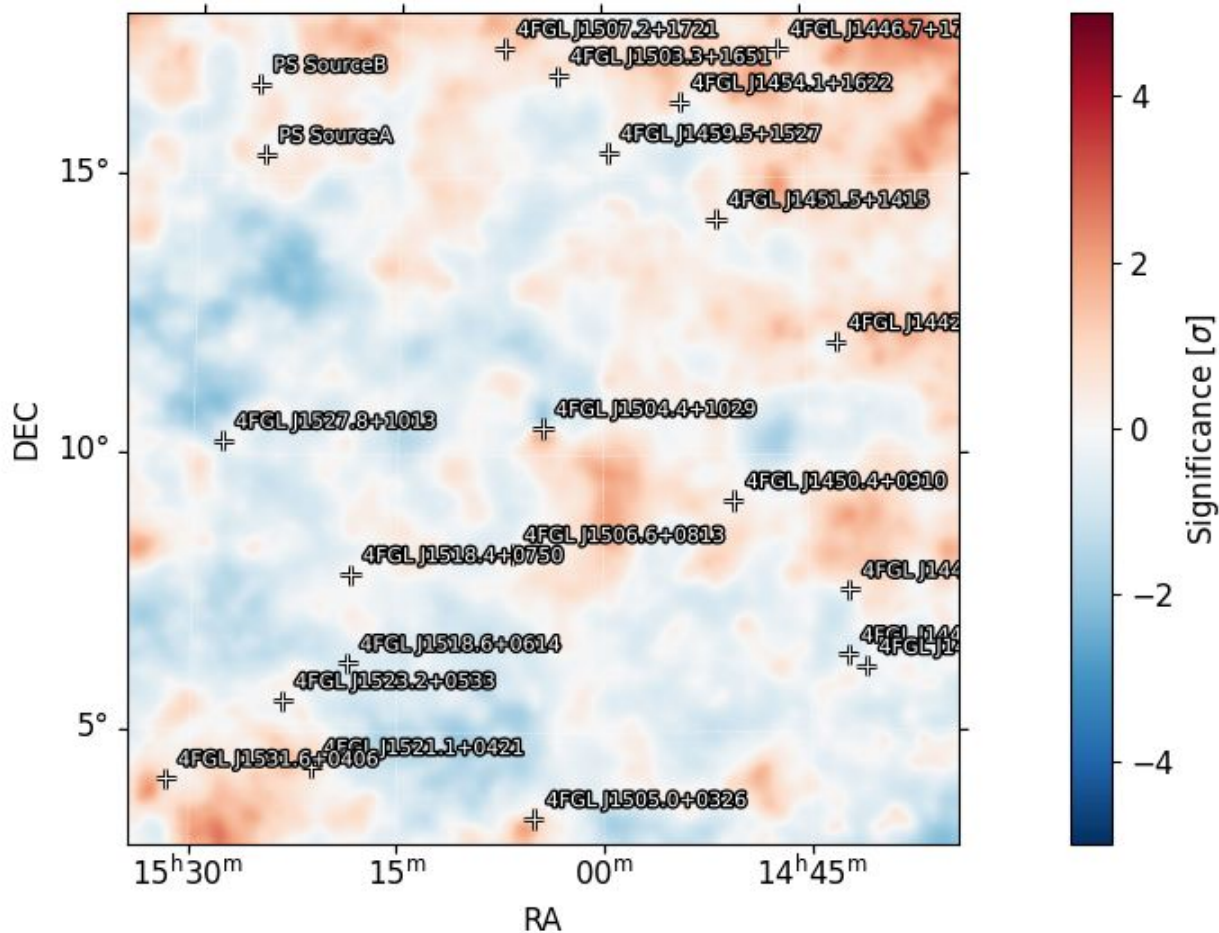
- Matched positions of point sources in the Fermi 4FGL DR2 catalog with track-type neutrinos from Giommi et al. (2020)
- Found 29 4FGL DR2 point sources, from which in case of 9 sources the predicted number of gamma-photons in 10 years is more than 1000 (5 BLL, 3 FSRQ, 1 SEY1)
- Generated the likelihood light curve of these gamma sources
- We see **IF** these AGN emit the neutrinos, neutrinos do not like to come during gamma-flares (4 after gamma flare, 1 before gamma flare, 1 at gamma flare, 1 between two gamma flares, 2?)
- If these AGN emit the neutrinos, they might be temporarily gamma-absorbed
- Theoretical works in this direction - results coming soon

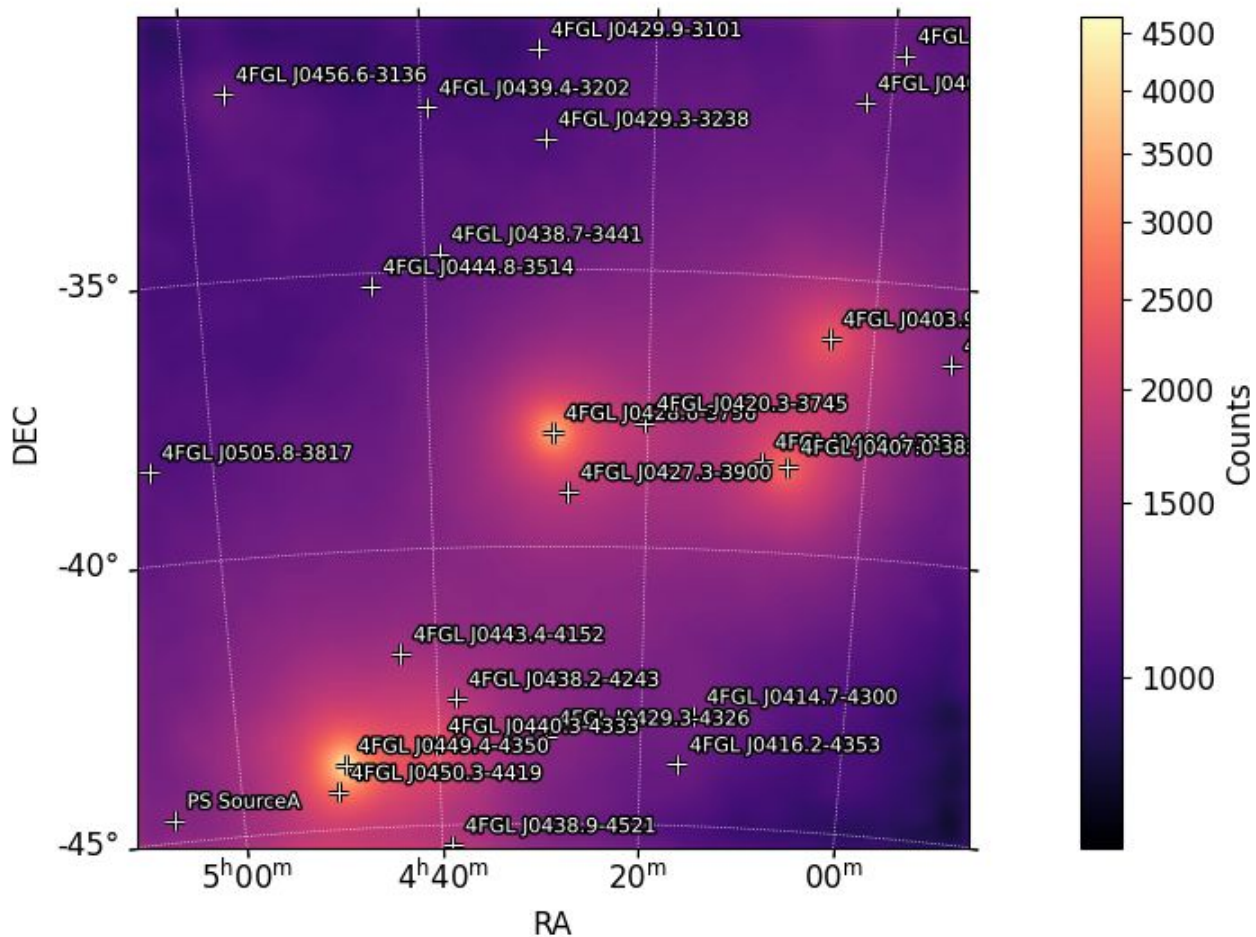
Thank you!

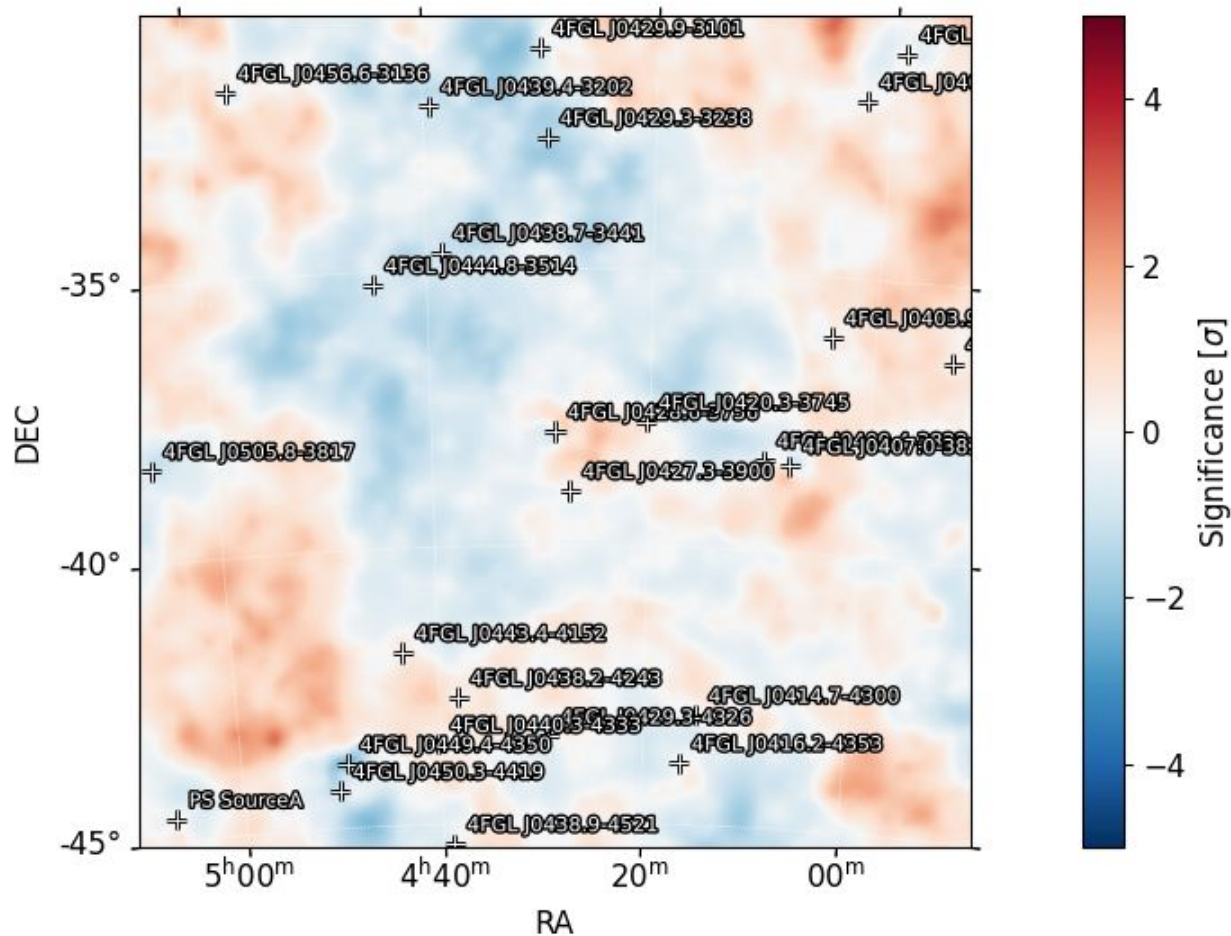


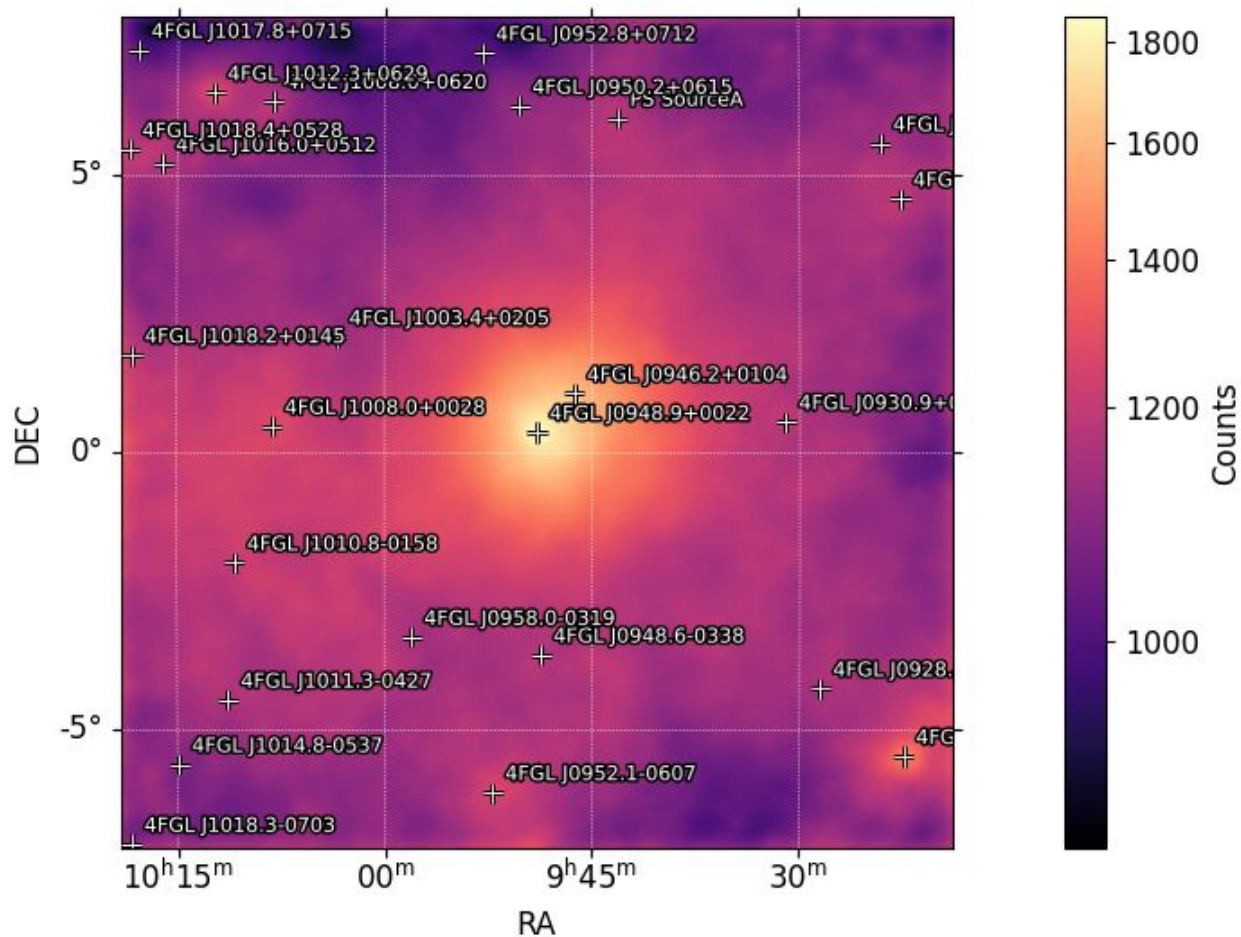




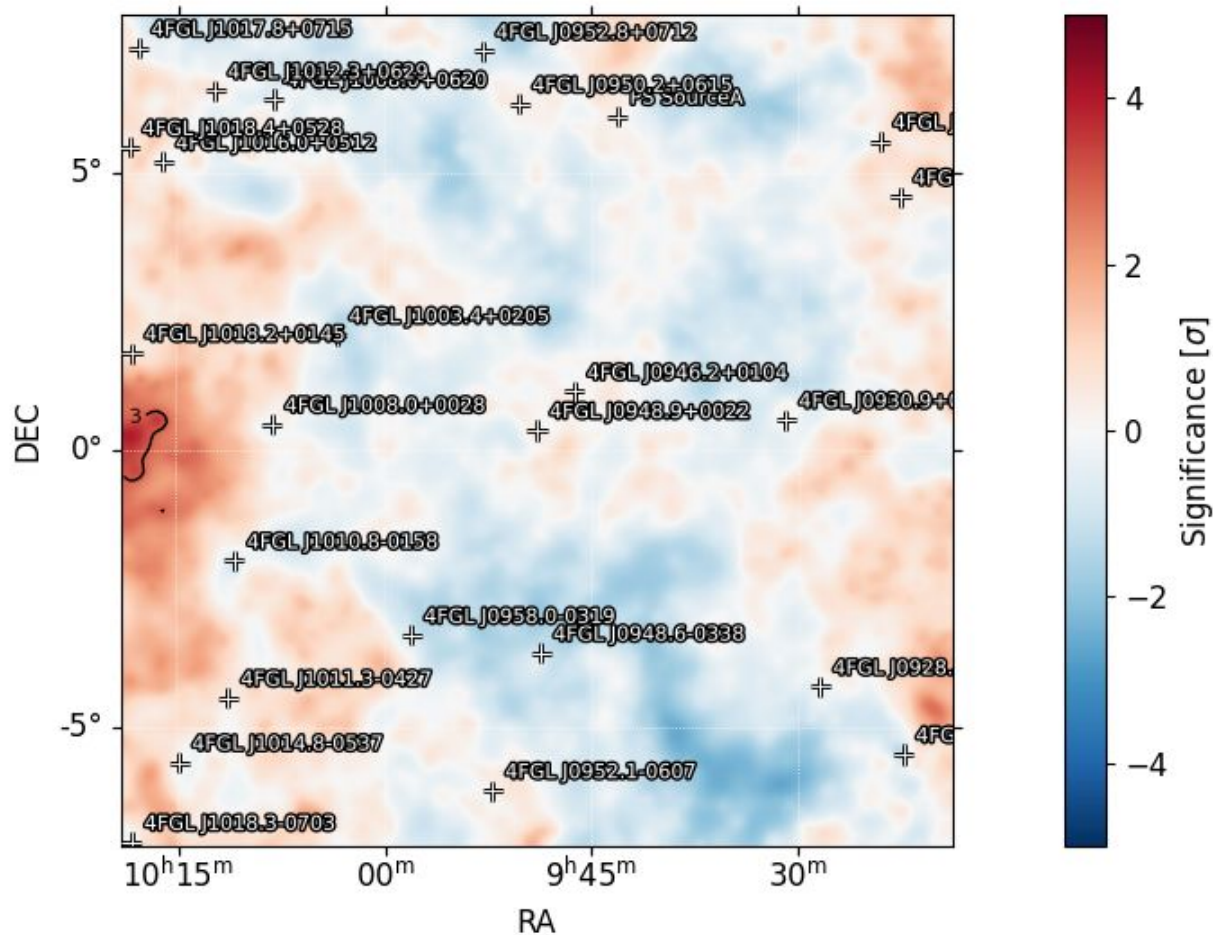


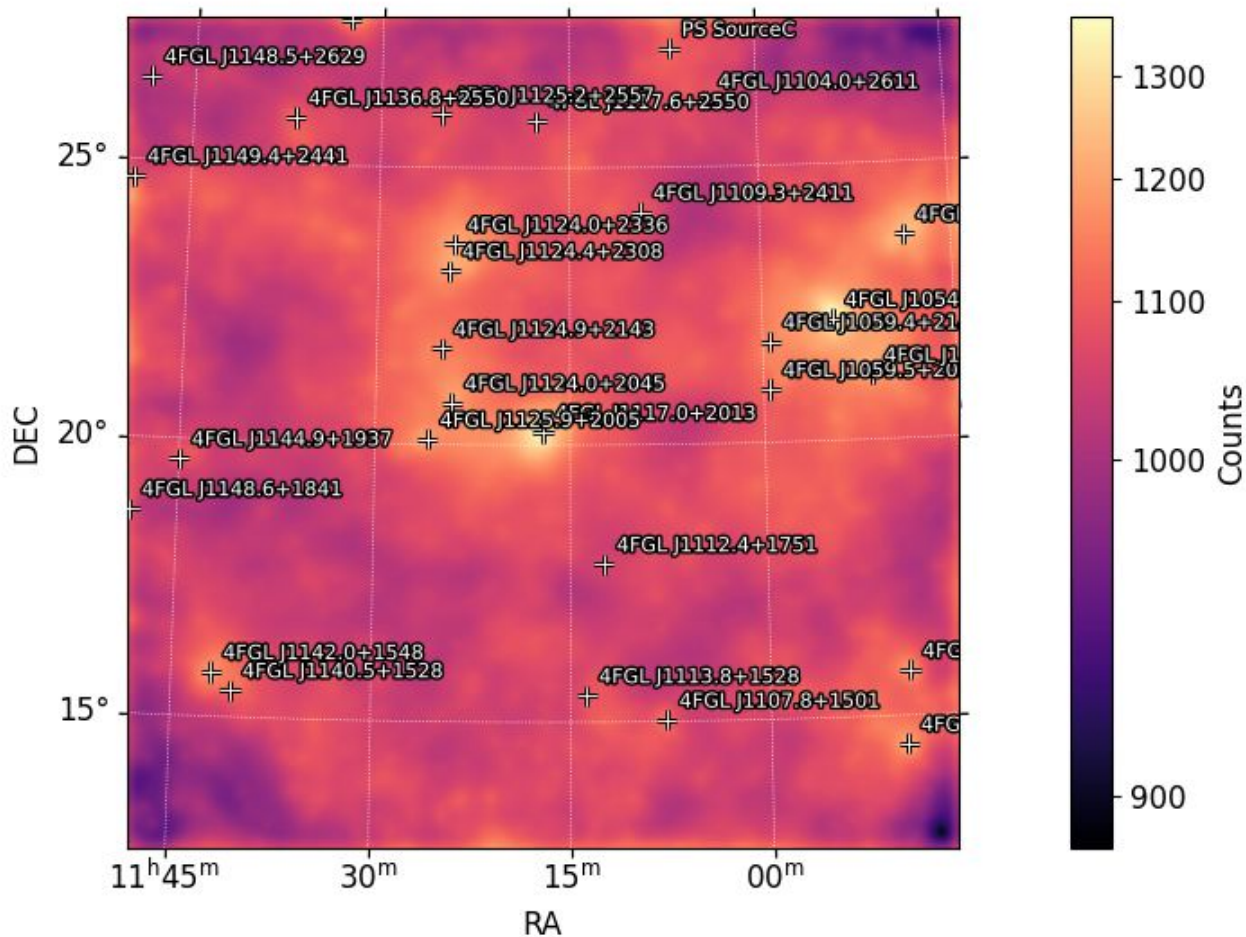


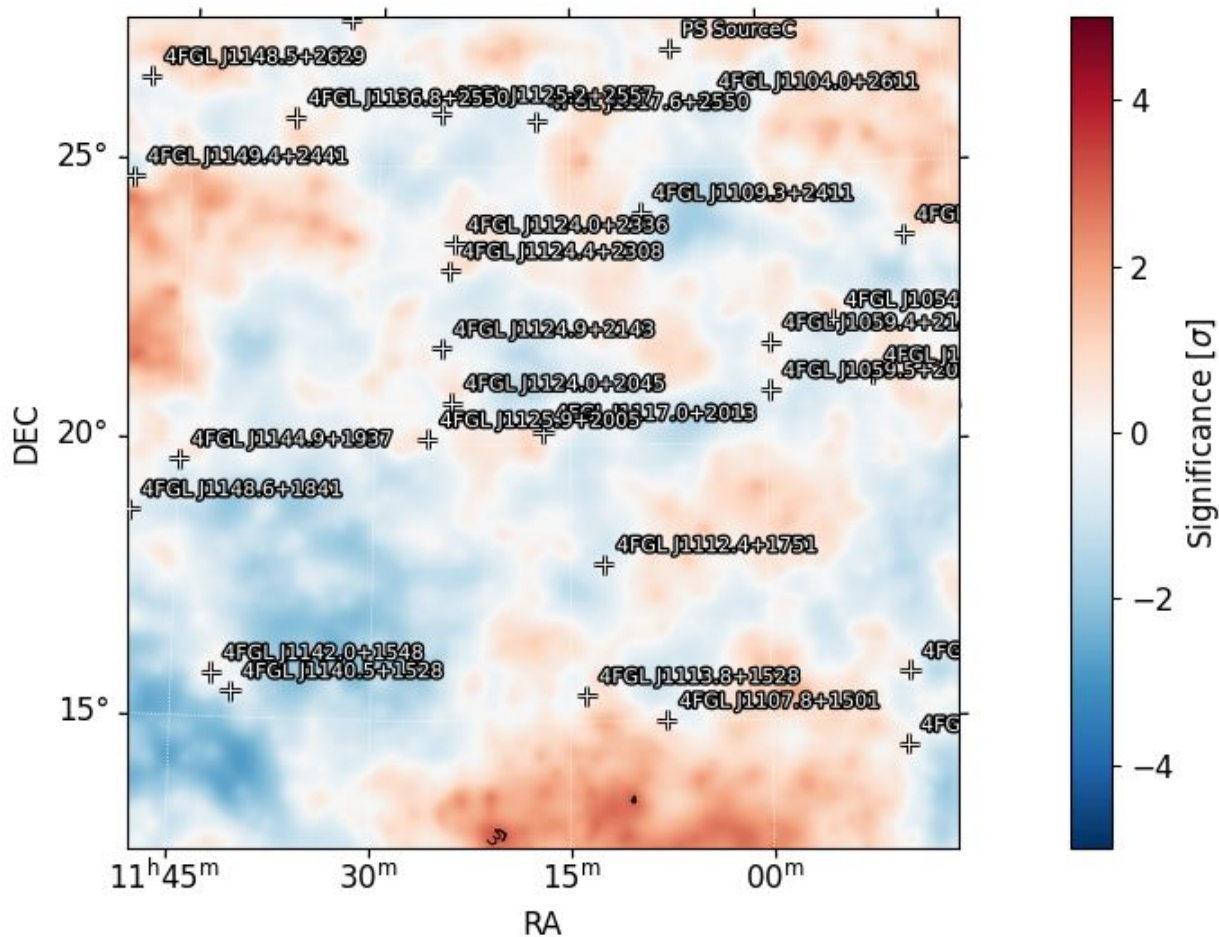


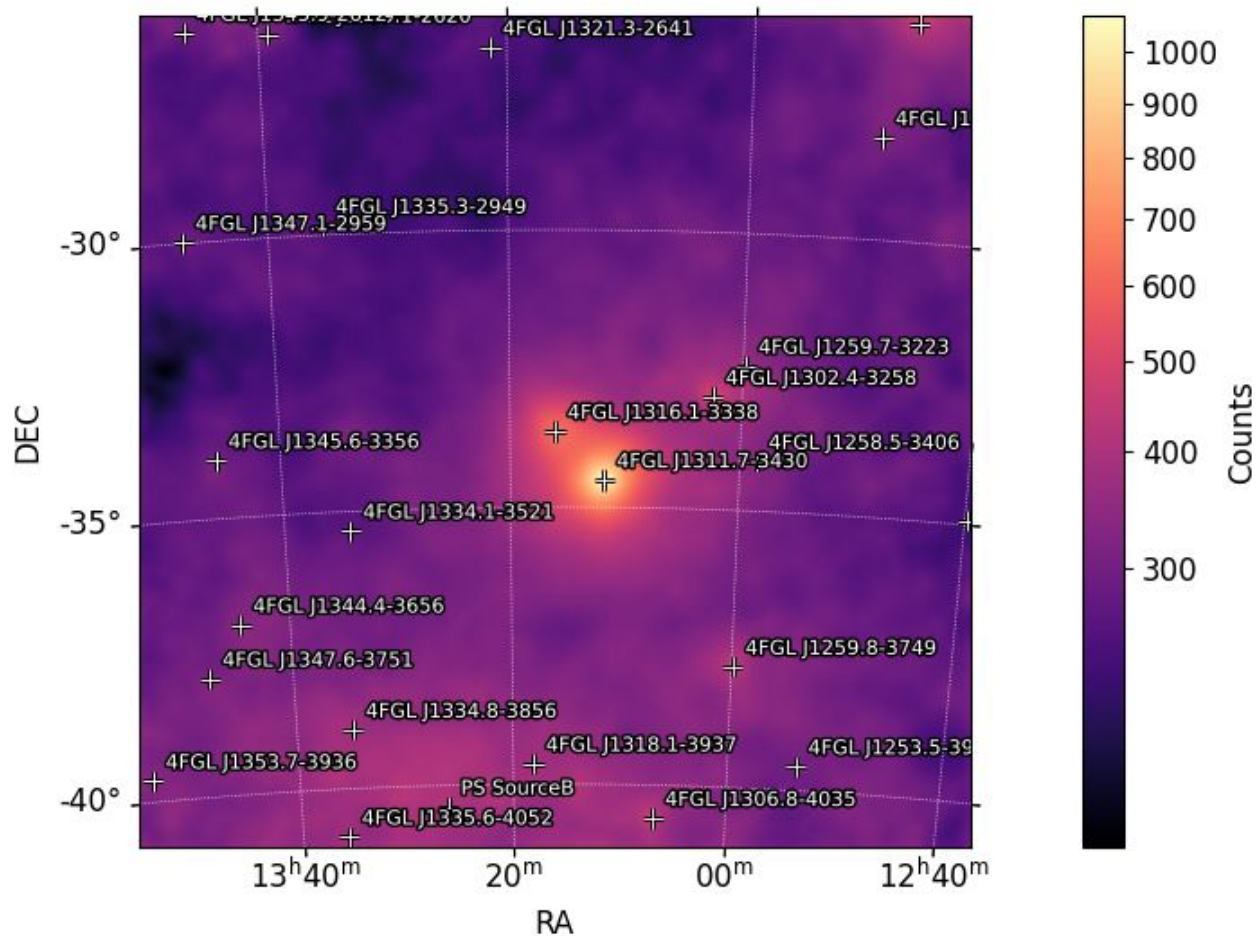


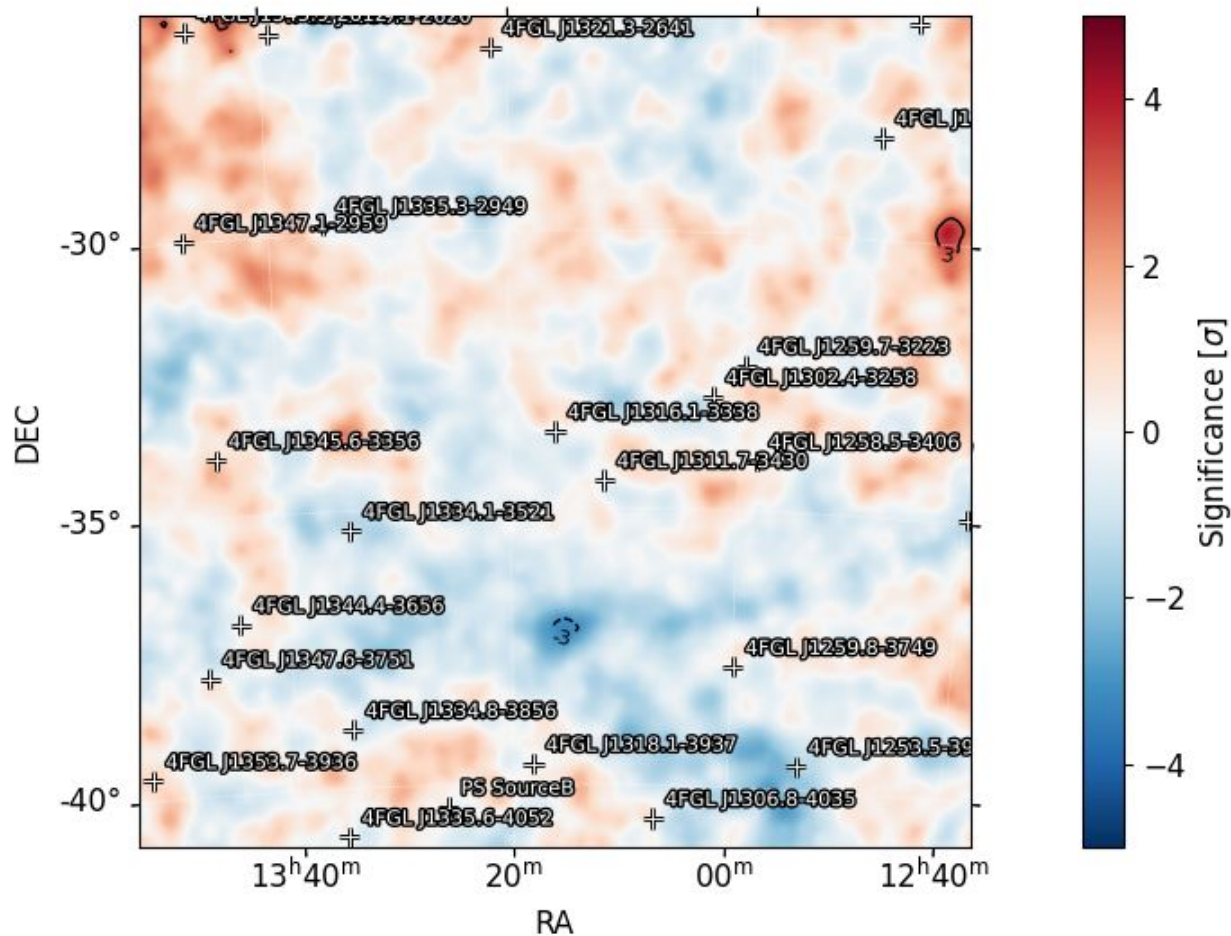
PMN J0948+0022 map of residual significance

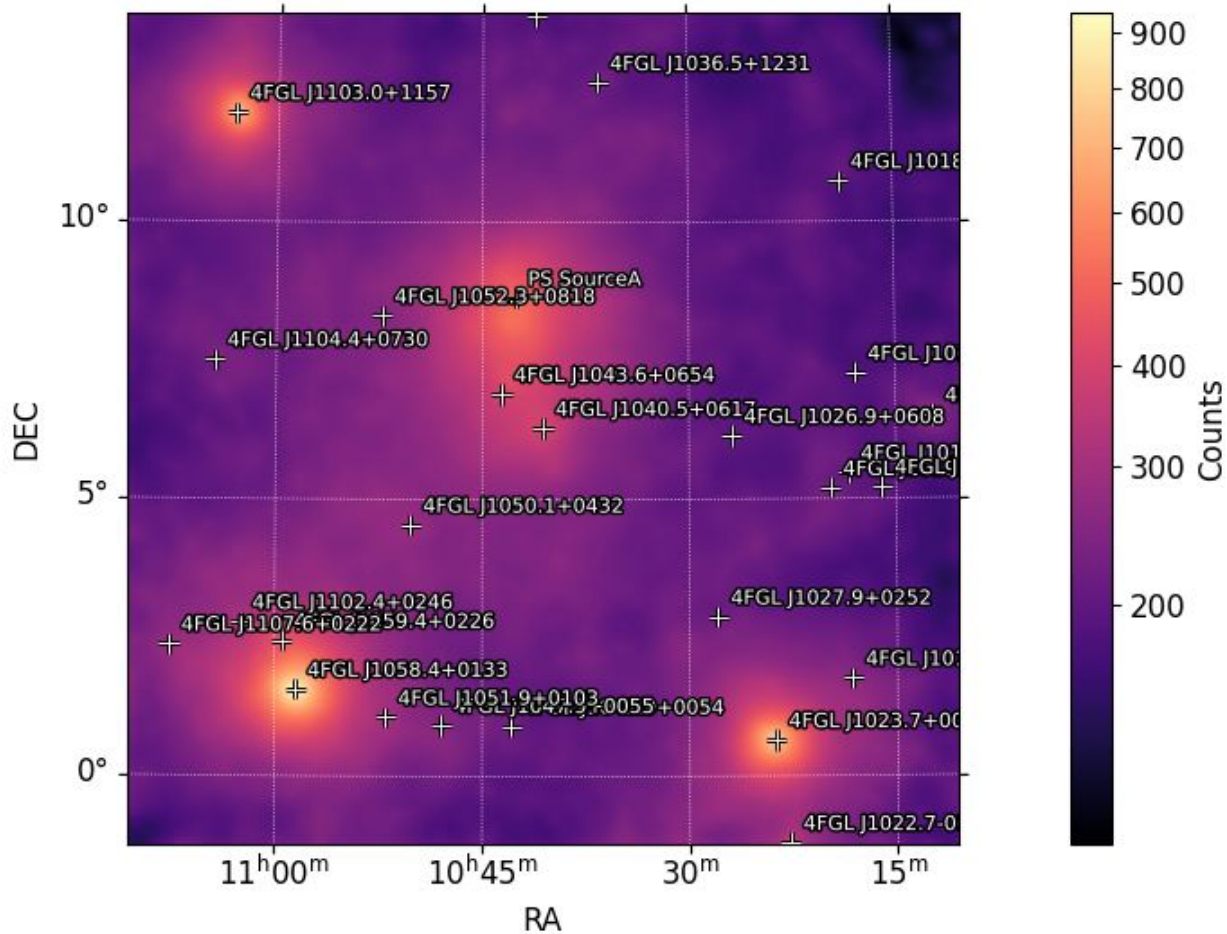




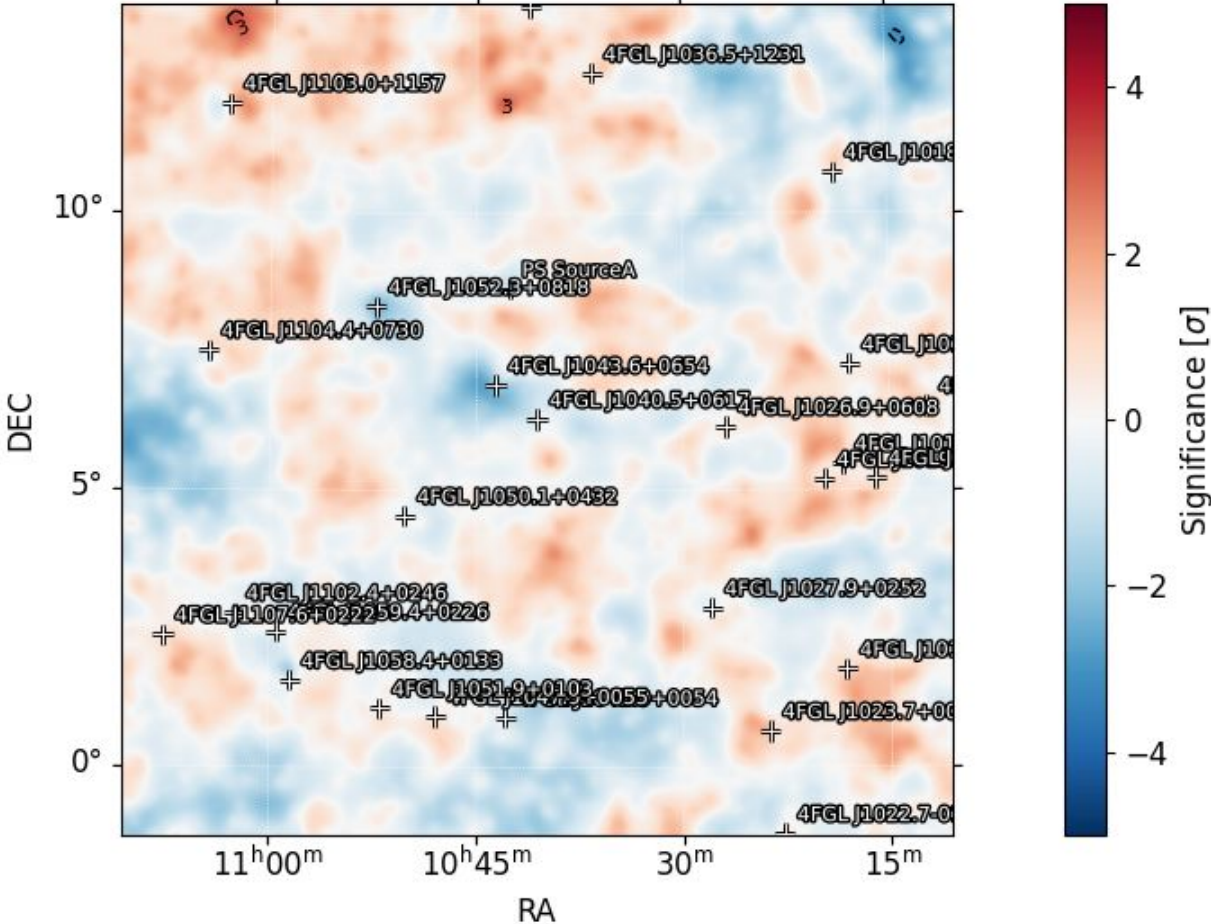


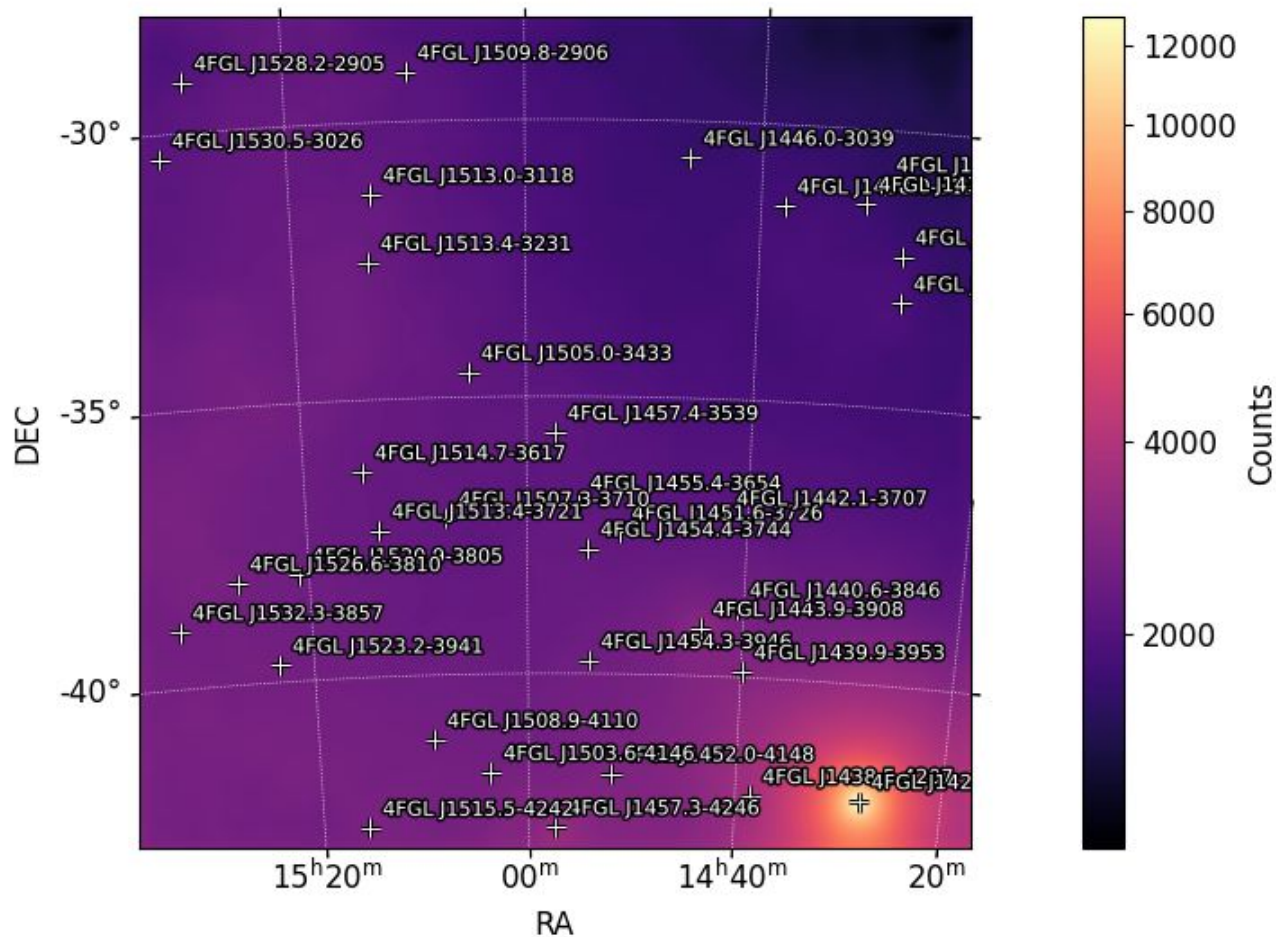


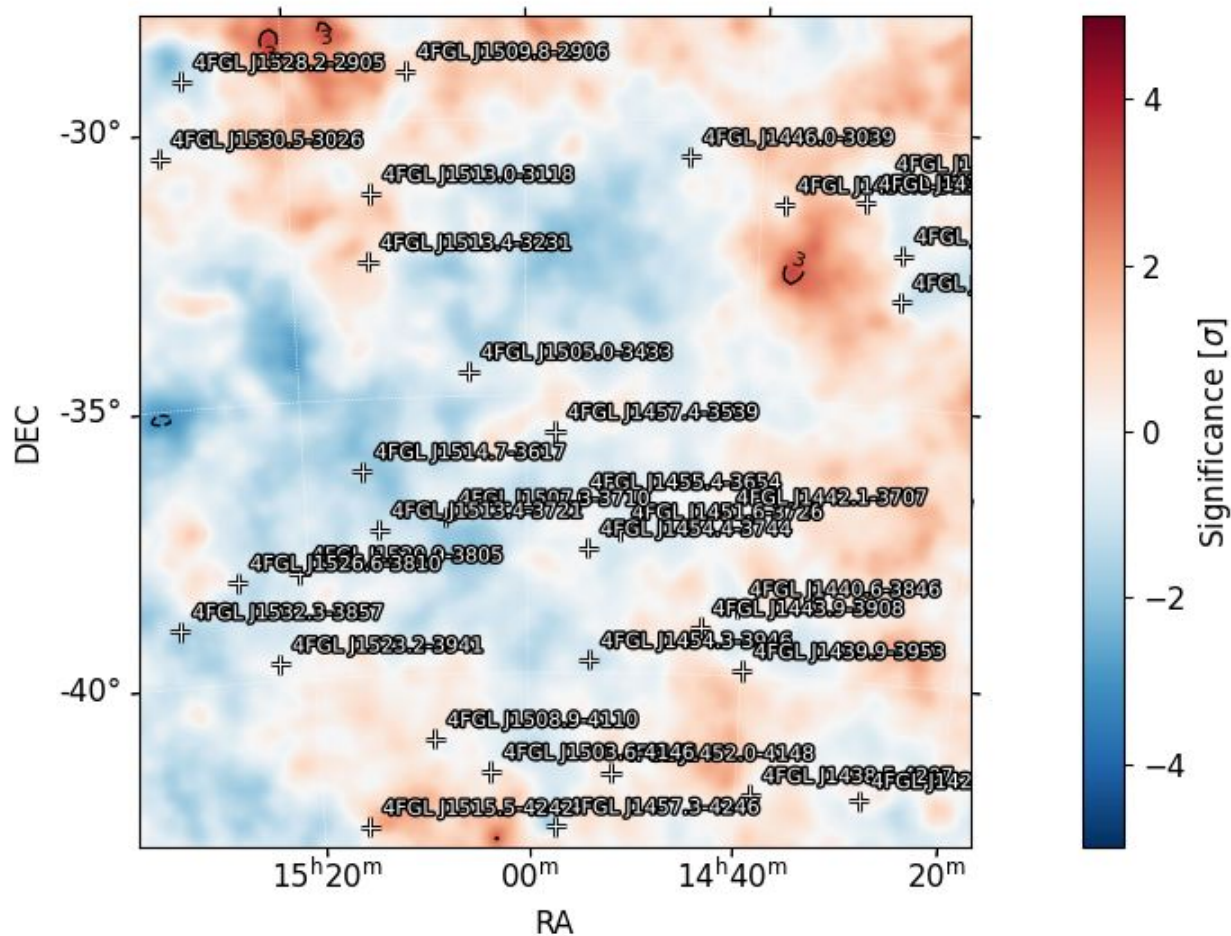




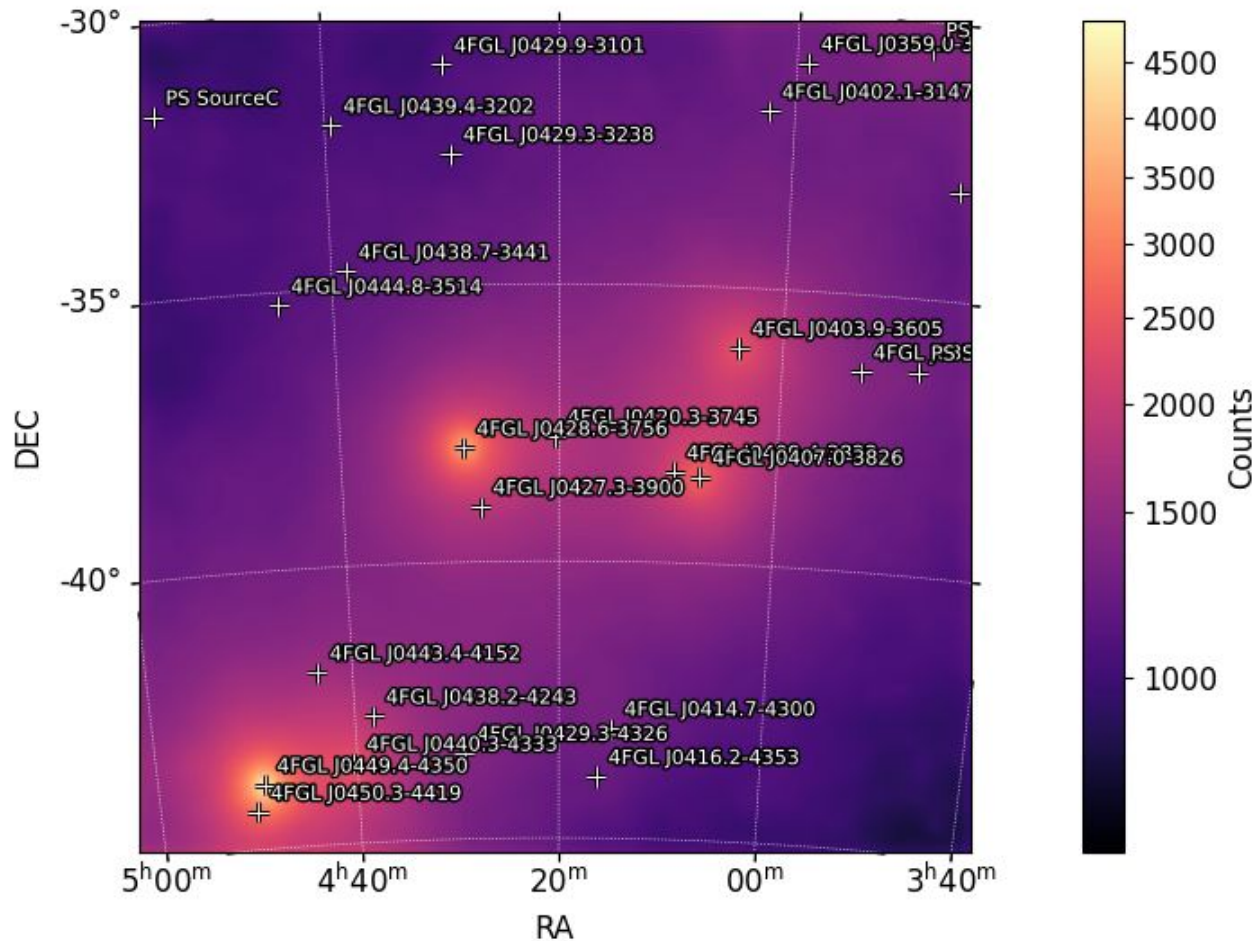
GB6 J1040+0617 map of residual significance







NVSS J042025-374443 smoothed data map



NVSS J042025-374443 map of residual significance

